American Mineralogist, Volume 76, pages 801–826, 1991

Polysomatism and polysomatic series: A review and applications

David R. Veblen
Department of Earth and Planetary Sciences, The Johns Hopkins University, Baltimore, Maryland 21218, U.S.A.

Abstract

The concepts of polysomatism and polysomatic series (Thompson, 1970, 1978) provide a basis for understanding the crystal structures, chemographic relations, structural disorder, and replacement reactions of many important families of rock-forming minerals and other crystalline solids. Polysomes are structures that can be created by combining two or more structurally and stoichiometrically distinct types of slab modules, and polysomatic series are groups of structures that are made up of different ratios of the same types of slabs. Many polysomatic structures can be described alternatively as crystallographic shear (CS) structures, as chemical twinning structures, or by other modular crystallographic models.

Numerous examples of polysomes are presented, illustrating various aspects of polysomatism. The CS structures of the ReO_3 and perovskite structure types are examined to show the relationships between the CS and polysomatic models. Polysomatic structures that have been described as periodic chemical-twinning (CT) structures include certain sulfosalts, oxyborates, the enstatite-IV series, and the humite group. Some polysomatic series possess a chain structure as one end-member and a sheet structure as the other, including the biopyriboles and the carlosturanite series. Antigorite samples having different modulation wavelengths are an example of a polysomatic series constructed from three different modules. The pyroxene-like regions of the manganese pyroxenoids are compared with the clinopyroxene structure as an illustration of the structural similarity of analogous slabs in different polysomes. The polysomatic model for sheet silicates has been used to generate structural models rapidly for computer simulation of electron microscopy images. The chain and sheet manganates provide examples of polysomes in which the stacking of slabs occurs in two dimensions; structures of this sort are called block structures by solid-state chemists.

The polysomatic model provides a basis for understanding the structural disorder, structural details, and chemical relationships among structures in a polysomatic series. Structural disorder based on mistakes in the slab sequence has been reported from virtually every polysomatic mineral group that has been investigated with transmission electron microscopy, and in some polysomatic series such structural disorder is rampant. Structures belonging to a polysomatic series are necessarily stoichiometrically collinear, and the polysomatic model provides a method for calculating the stoichiometry (i.e., the structural formula) even in structurally disordered regions of a crystal. The details of polyhedral distortions and chemical partitioning may be very similar in structurally analogous crystallographic sites throughout a polysomatic series, providing a method for predicting these factors; the CS and chemical twinning models do not afford this advantage.

Reactions in which one polysome replaces another are common and geologically important. Typically in such reactions, one sequence of polysomatic slabs is replaced by another. The description of the reaction mechanism by the polysomatic model is simple and not only implies the structural displacement involved in the reaction (which in some cases may be described alternatively as the propagation of a dislocation), but it also describes the details of the beginning and final states in the reaction. Such a description is therefore more complete than descriptions based on the dislocation alone and also provides a uniform description for those polysomatic reactions that involve no net shear. The terminations of polysomatic slabs are the sites at which chemical reactions actually take place. These terminations inherently are linear zones of structural disruption and commonly are tunnels with free apertures similar to those found in zeolites. It is argued that bulk diffusion is much too slow to account for the chemical changes that occur in many polysomatic reactions and that most chemical transport that takes place in such reactions therefore must occur at the terminations of the advancing polysomatic slabs. Zeolite-like

0003–004X/91/0506–0801$02.00

diffusion rates at the terminations of the polysomatic slabs would be sufficient to account for the observed chemical transport in polysomatic reactions.

Introduction

The crystal structures of many rock-forming minerals and other compounds are complex. While it is essential for those working with the details of crystal chemistry and the thermodynamics of crystalline solutions to understand a structure on a site-by-site basis, many important processes in crystalline solids can best be visualized by breaking complex structures into larger modules containing many sites. One of the most powerful concepts in modular crystallography is polysomatism, as developed by J. B. Thompson, Jr. (1970, 1978, 1981a), to whom this volume is dedicated. This concept recognizes the fact that any crystal structure can be sliced into slabs. Furthermore, in some fortuitous cases, the slabs of one structure can be combined with the slabs of another structure. The resulting hybrid structures are called polysomes, from the Greek roots meaning many parts (Thompson, 1978; more graphically, Thompson also refers to them as "mineralogical mules").

Among the rock-forming minerals, there are numerous examples of polysomatism and of polysomatic series—groups of polysomes formed by mixing two or more different types of structural slab in different ratios. As pointed out by Thompson (1978), the pyroxenes, amphiboles, and micas form such a series, as do the minerals of the humite group, the pyroxenoids, and many sheet silicates. In the world of nonmineral crystalline materials, there are also numerous examples of polysomatic series, some of which are based on the geophysically important perovskite and rutile structures. Indeed, some of the new structural families of high-temperature superconductors are readily interpreted in terms of a polysomatic model.

The purpose of this paper is to review the concept of polysomatism, not exhaustively, but anecdotally. I will explore (1) the meaning of and requirements for polysomatism; (2) other types of modular crystal structures and alternative ways of describing polysomatic structures (e.g., crystallographic shear models); (3) selected examples of mineralogical polysomatic series that illustrate various facets of polysomatism and alternative descriptive models; (4) the utility of the polysomatic model for understanding structural disorder, the chemographic relationships among polysomes, and the details of polyhedral distortions and chemical partitioning in polysomatic structures; and (5) the use of the polysomatic and crystallographic shear models for understanding the mechanisms of solid-state reactions. It is not my intention to review the full range of polysomatic structures exhaustively, because they probably number in the thousands. Instead, I will provide selected examples that elucidate the many uses of the polysomatic model in crystal chemical, mineralogical, and petrological relations. Where appropriate, I will use results from high-resolution transmission electron microscopy (HRTEM) experiments to illustrate polysomatic structures (for a review of HRTEM in mineralogy, see Buseck and Veblen, 1988).

What is polysomatism and what are polysomatic series?

The concept of polysomatism can be understood by referring to Figure 1 or a set of child's colored building blocks—the beauty of this concept is its simplicity. Figure 1a shows a cross section through a hypothetical crystal structure called A, which has been sliced into a series of slabs, also labeled A. Figure 1b shows a second structure, B, sliced into slabs labeled B; it is assumed that A and B possess different structures and stoichiometries. Figure 1c shows a third structure that has been constructed from the A and B slabs by alternating them rigorously in the sequence . . . ABABABAB . . . . This structure can be indicated by the symbol (AB), where the parentheses indicate that the unit AB is repeated periodically. The structure (AB) is a polysome, or polysomatic structure, formed from the end-member structures (A) and (B); the unit cells of most polysomes contain either one or two of the repeating units. Similarly, another polysome, (ABB), is illustrated in Figure 1d. Together, the structures (A), (AB), (ABB), and (B) form a polysomatic series.

An obvious consequence of polysomatism is that all the members of a polysomatic series will be stoichiometrically collinear (where the stoichiometry refers to the formula unit written in terms of crystallographic sites, rather than their specific chemical inhabitants). For example, the stoichiometries of all the polysomes shown in Figure 1 are linear combinations of the stoichiometries of the A and B slabs. This is not to say that the detailed chemical compositions of all polysomes of a series are required to be collinear, as discussed in the section on polyhedral distortions and chemical partitioning. Specifically, if the minerals of a polysomatic series contain more than two chemical components, then the stoichiometric collinearity does not require chemical collinearity.

What are the structural requirements for forming a polysomatic series?

Although any structure can be cut into an assembly of identical slabs (e.g., slabs the width of the unit cell), it is not possible to form a polysomatic series from most arbitrarily chosen pairs of structures. For example, there are no known structures that can be represented as polysomatic mixtures of quartz slabs and hematite slabs. What, then, determines which structures can mate to form these mineralogical mules?

An obvious requirement for forming a polysome is that the energy of the interfaces between the component slabs must not be too great. In simple structural terms, this requires that there be structural continuity between the slabs—when they are joined together, there should be no

dangling bonds. This rather severe constraint implies that the two end-member structures of a polysomatic series must possess quasi-planar surfaces with very similar structures and lattice translations that are nearly equal or equal to integral multiples of each other. At first glance, the requirement for nearly identical two-dimensional structures may seem to be insurmountable. Because O-O distances and the arrangement of O ions in planar arrays are similar for many O-based compounds, however, there are some pairs of structures that can be sliced into slabs that fit together almost perfectly. It is such pairs that form polysomes.

Although sharing of symmetry may not be a rigorous requirement for the formation of polysomes, the mating surfaces of polysomatic slabs typically do have the same plane-group symmetry. Indeed, the topic of slab symmetries and the way they combine to form the overall space-group symmetry of polysomes and polytypes has received much attention, particularly with respect to the biopyribole series. Although these symmetry aspects of polysomatism are beyond the scope of this review, the reader is directed to the papers by Thompson (1978, 1981a, 1981b), Cameron and Papike (1979), Law and Whittaker (1980), Chisholm (1981), and Hawthorne (1983).

Interaction energies among the constituent slabs of a polysome have been used by some authors to simplify the calculation of structure energies. For example, Price and Yeomans (1984, 1986) argue that the stabilities of a wide range of polysomatic and polytypic structures can be rationalized in terms of the interactions between first and second nearest-neighbor slabs, using the ANNNI (axial next-nearest-neighbor ising) model. Such approaches have been applied to a variety of modular crystal structures, including biopyriboles, pyroxenoids, minerals of the humite group, spinelloids, carbonates, and sheet silicates (e.g., Price and Yeomans, 1984, 1986; Price, 1983; Angel et al., 1985).

Modular crystal structures and their description

The concept of modular crystallography is based on the observation that the same or similar structural fragments can appear in more than one crystal structure. These fragments may consist of clusters of atoms or coordination polyhedra and can be finite units, one-dimensionally infinite rods, or two-dimensionally infinite slabs. Modular crystallography is important for simplifying the visualization of crystal structures, for understanding the relationships among various structures, and for understanding the thermodynamic stabilities of crystalline compounds (Hazen and Finger, 1981; Price and Yeomans, 1986).

Different approaches to modular crystallography

The crystal structures of chemical compounds can be viewed in many ways, for example, as arrays of coordination polyhedra of anions around cations (Pauling, 1929).

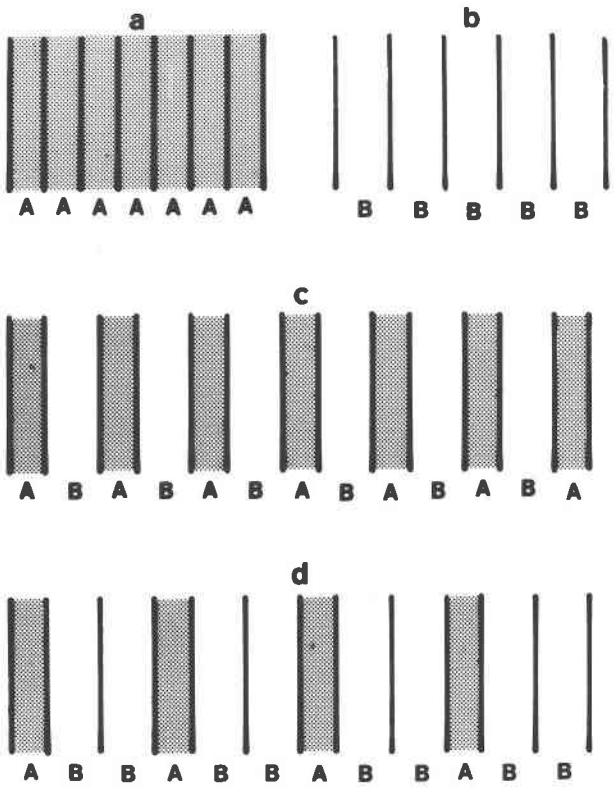

Fig. 1. Schematic diagrams illustrating polysomatism. (**a**) The structure (A), made up of A slabs. (**b**) The structure (B), consisting of B slabs. (**c**) The polysome (AB). (**d**) The polysome (ABB).

Alternatively, O'Keeffe and Hyde (1985) view structure in terms of cation packing, preferring to describe O-based materials as stuffed derivatives of alloys or intermetallic compounds. One approach to the simplification and systematization of crystal structure is to classify structures according to the topology of nets formed by interlinked polyhedra (e.g., Liebau, 1985; Smith, 1977, 1978, 1979; Hawthorne, 1985). A related approach is to define modules of linked polyhedra that occur in more than one crystal structure. Such units have been called fundamental building blocks, or fbb's (e.g., Moore et al., 1985; Moore, 1986), and they can comprise isolated fragments, rods, or sheets. The structures of zeolites are commonly described in terms of such fragments that include various types of ring and cage units (Breck, 1974, ch. 2). In many cases, alternative descriptions are possible. For example, Moore et al. (1985) describe the structures of lawsonite, sursassite, macfallite, pumpellyite, julgoldite, ardennite, orientite, ruizite, santafeite, and bermanite with a fbb model, whereas Ferraris et al. (1986) describe these structures in terms of polysomatism and polytypism.

Modular structures can be described further by noting the ways in which the modules are packed or stacked together or with other modules. For example, O'Keeffe and Andersson (1977) noted that many structures (e.g.,

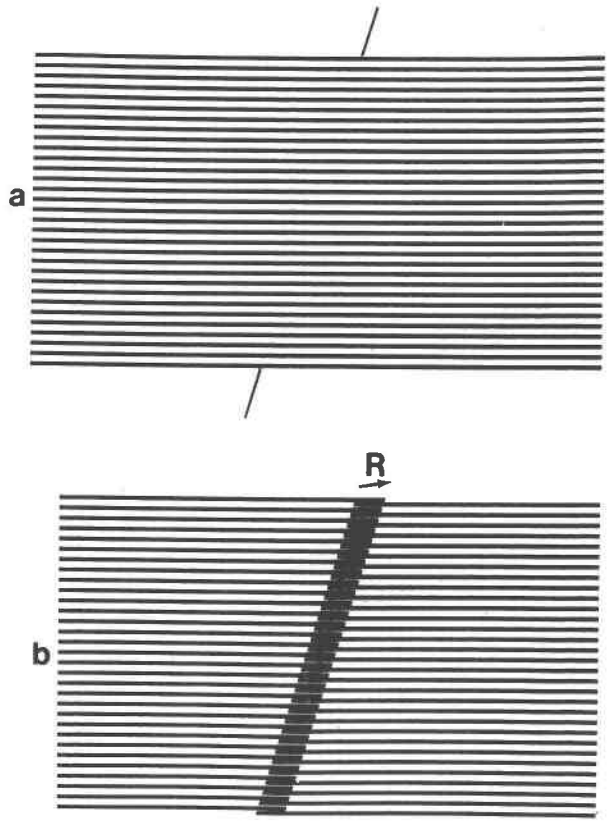

Fig. 2. The operation of crystallographic shear (CS). (**a**) The parent structure is cut along a plane indicated by the two inclined lines. (**b**) The structure on one side of the cut is displaced relative to that on the other by a displacement vector, **R**, that is not parallel to the plane of the cut. The crystal structure in the region of the shear plane is now different from that of the parent structure and has a different stoichiometry.

garnet) can be rationalized in terms of the packing of structural rods. In some cases, modular descriptions have bordered on the bizarre, as in the elucidation of the "elephantine" unit cell of the "balosilicate" ashcroftine as consisting of a central, ordered "curd" surrounded by an encrusting border "limbus" and an encasing disordered "whey" (Moore et al., 1987). As different as they are, the unifying theme of such descriptions is that they seek to simplify and rationalize complex structures.

Description of mixed-module layer structures

Any crystal structure can be viewed as a layer structure, simply by defining infinite slabs that are one unit cell thick. However, it is traditional to view only those structures with weakly bonded layer modules or with two very different types of structural slabs as layer structures. Crystals consisting of layer modules that are structurally and chemically identical or very similar are defined as polytypic (Bailey et al., 1977; Guinier et al., 1984); polytypism is a relatively simple concept and is discussed in the next section. On the other hand, crystals consisting of layers that are structurally or chemically distinct, or both, can be described in a number of different ways, as pointed out by numerous authors (e.g., Thompson, 1978; Tilley, 1980; Angel, 1986a).

Homologous series. This term is used to describe chemically collinear groups of molecules or crystalline compounds. Although the first use of this term in crystallography was to describe crystallographic-shear derivatives (see below) of the rutile structure type, in present usage it does not imply any specific structural phenomenon. Instead, the term is sometimes used to refer generically to the various types of intergrowth structures described in this section (e.g., Hazen and Finger, 1981).

Crystallographic shear structures. A crystallographic shear (CS) plane is a region that could be produced by cutting the crystal along an oriented surface (Fig. 2a) and then displacing, or shearing, the two parts of the structure by a vector that is not parallel to the plane of the cut (Fig. 2b). (Displacements parallel to the plane of the cut would produce a stacking fault or antiphase boundary.) The sense of shear can be either compressional or dilatational. If a CS plane is isolated within the crystal, it is considered to be a planar defect and is sometimes called a Wadsley defect, after the solid-state chemist who first recognized crystallographic shear as a structural principle (Wadsley, 1964). Alternatively, CS planes can be repeated periodically, forming ordered compounds called CS structures. If the CS planes occur in two different orientations, the result can be called a block structure.

In the region of a CS plane, the linkage of coordination polyhedra is altered (e.g., corner sharing can become edge sharing, or vice versa), and the stoichiometry of the crystal is altered. CS planes thus provide a mechanism for accommodating nonstoichiometry, for example, in vacancy-intolerant simple oxides. Such is the case in whole families of CS structures based on the ReO_3, rutile, and Nb_2O_5 structure types. While CS planes actually can form by shearing of a preexisting crystal, as in some reduction reactions, they also can form during crystal growth. The mere presence of a defect that can be described as a CS plane therefore does not necessarily imply a shearing mechanism for reaction that produced the defect or even that the defect was produced by a reaction. Because of their importance in solid-state chemistry, there are several excellent reviews of CS structures (Anderson, 1972; Tilley, 1980, 1987; Eyring, 1988), including one devoted to silicates (Chisholm, 1975).

Chemical twinning. This term is used to describe defects and structures similar to CS planes and CS structures. Again, the parent structure (Fig. 3a) is severed along planar surfaces, but it is reconstructed by a twinning operation, rather than shearing (i.e., the operation relating the material on one side of the plane to that on the other is a point-group operation, rather than a translation). In the region of the twin plane, crystallographic sites are altered or new sites are produced that may accommodate elements typically not present in the parent structure (Fig. 3b). If the twin planes occur periodically, a homologous

series results, with the stoichiometry depending on the spacing between these planes. Examples of structures produced by chemical twinning are given by Andersson and Hyde (1974), O'Keeffe and Hyde (1985), Tilley (1987), and Eyring (1988); the review by Takéuchi (1978) concentrates on several mineralogical examples. The term "nonconservative twin" has also been used to describe the chemical twinning operation (Van Landuyt et al., 1974).

Crystallographic purists may well object to the use of the term "twin" in describing these structures. Indeed, a twinning operation by definition cannot be a symmetry operation of the untwinned material, yet the operation involved in these chemical twinning structures typically is a symmetry operation in the resulting structure. However, the term "chemical twinning" has gained widespread usage in the field of solid-state chemistry to the point that the acronym "CT structure" is common currency. It will be used here, therefore, to facilitate comparisons between the chemical twinning and polysomatic models.

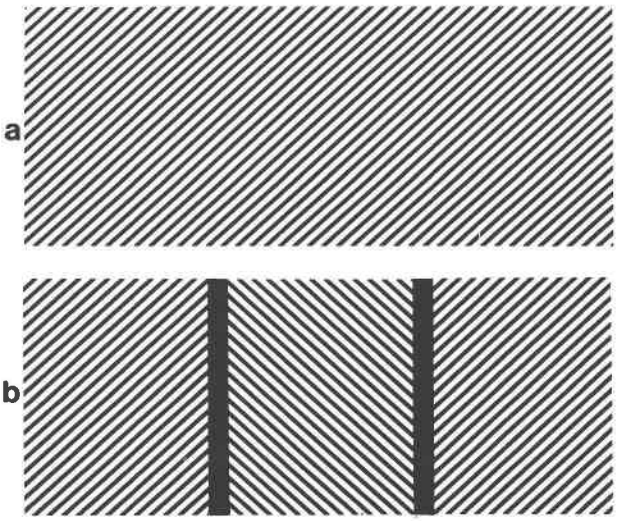

Fig. 3. Chemical twinning (CT). (**a**) The parent structure from which the CT structure will be derived. (**b**) The structure after inserting twin planes. The crystal structure along the twin planes is altered compared to that of the parent structure, as indicated by the heavy black lines, and has a different stoichiometry.

Polysomatism, mixed-layer polytypism, and heteropolytypism. These terms, coined by Thompson (1978), Kohn and Eckart (1965), and Warshaw and Roy (1961), respectively, refer to similar phenomena involving the mixing of more than one type of structurally and chemically distinct module, as explained in the section defining polysomatism and in Figure 1. The terms are not perfectly synonymous, however, because the polysomes of a polysomatic series can possess different ratios of the two slabs, leading to a variety of stoichiometries, whereas the members of a group of mixed-layer polytypes all have the same ratio of slabs and hence the same stoichiometry (Kohn and Eckart, 1965).

Polytypism

Polytypism has been defined similarly by two International Union of Crystallography (IUC) nomenclature committees (Bailey et al., 1977; Guinier et al., 1984): "An element or compound is *polytypic* if it occurs in several different structural modifications, each of which may be regarded as built up by stacking layers of (nearly) identical structure and composition, and if the modifications differ only in their stacking sequence. Polytypism is a special case of polymorphism: the two-dimensional translations within the layers are (essentially) preserved whereas the lattice spacings normal to the layers vary between polytypes and are indicative of the stacking period. No such restrictions apply to polymorphism." For the present review, this definition will be followed, and the term polysome will be reserved for compounds in which the slab modules have substantially different structures, stoichiometries, or both (Thompson, 1978).

Angel (1986a) pointed out several difficulties with the above definition of polytypism, primarily related to the permissible ranges in chemical and structural variation allowable within the definition. This clearly is a valid area for debate. Note that in defining polysomatism, I simply stated that the modules are different, without defining precisely what different means. Although the IUC committees (Bailey et al., 1977; Guinier et al., 1984) have defined permissible compositional ranges and explained the permissible types of structural variation for polytypes, Angel (1986a) notes correctly that the compositional limits are arbitrary and nonuniform from structure to structure, and structural variation is not quantified.

Because of these difficulties in defining polytypism rigorously, Angel (1986a) argued that the definition of polytypism should be expanded greatly, to encompass all types of two-dimensional modular structure described above, including polysomes. I do not agree with Angel's proposal. Although points of nomenclature can be debated ad infinitum without resolution, the classical separation between polytypes and polysomes has been useful in practice. There probably will always be some debate over whether certain borderline structures are classical polytypes or polysomes. However, this problem of classification is not alleviated by treating polysomatism as a subset of polytypism, as in the scheme of Angel (1986a), which classifies layer-module structures as type I polytypes (classical, single-module structures) or mixed-module polytypes that include type II (constant module ratio), type IIIa (variable ratio, constant stoichiometry), and type IIIb (variable ratio and stoichiometry). The classification problem simply shifts to the question of what type of polytype a specific structure is. In addition, if Angel's (1986a) scheme is followed, one is faced with the fact that many structures are simultaneously both type I and type IIIb polytypes. As a result, in the present review I call Angel's type I structures polytypes and his type II and III structures polysomes.

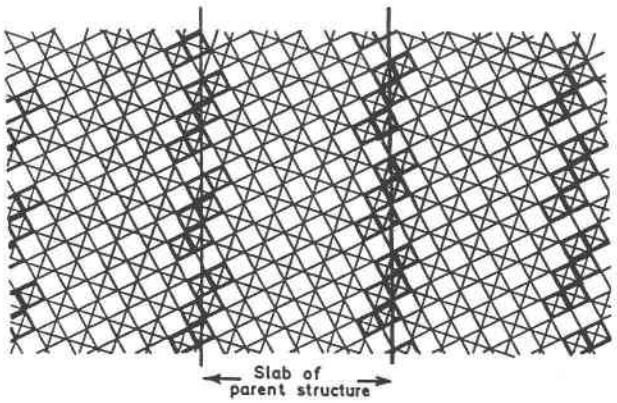

Fig. 4. The structure of $W_{20}O_{58}$, which is derived from the WO_3 structure by the insertion of periodic crystallographic shear planes. Between the CS planes are slabs of the parent WO_3 structure, in which the WO_6 octahedra share corners. Octahedra along the CS planes share edges. (From Anderson, 1972.)

Examples of polysomatic series

In this section, I will explore several examples of polysomatic structures and series, with the goal of illustrating some of the important features of polysomatism.

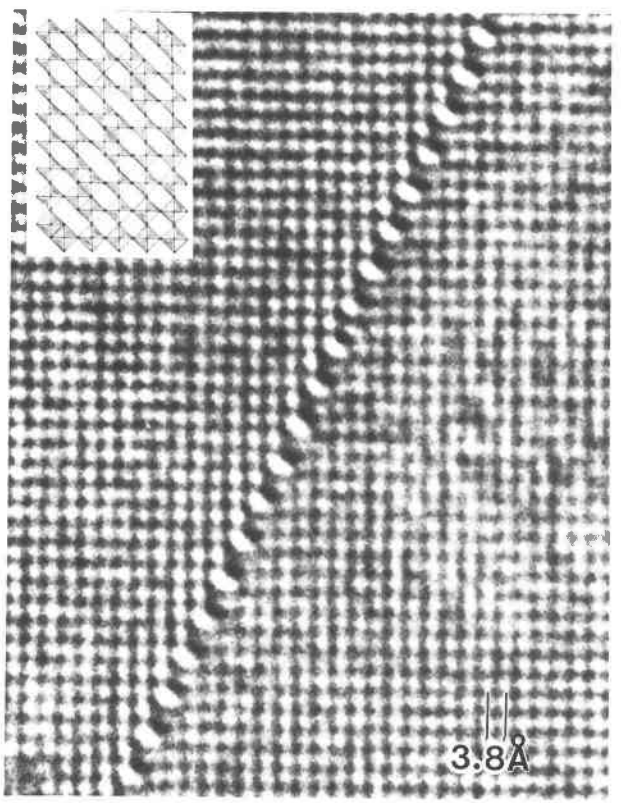

Fig. 5. An isolated CS plane formed by a reduction reaction in WO_{3-x}. By sighting at a low angle along either the vertical or horizontal direction, it can be seen that the structure on one side of the fault has been displaced relative to that on the other. (After Iijima, 1975.)

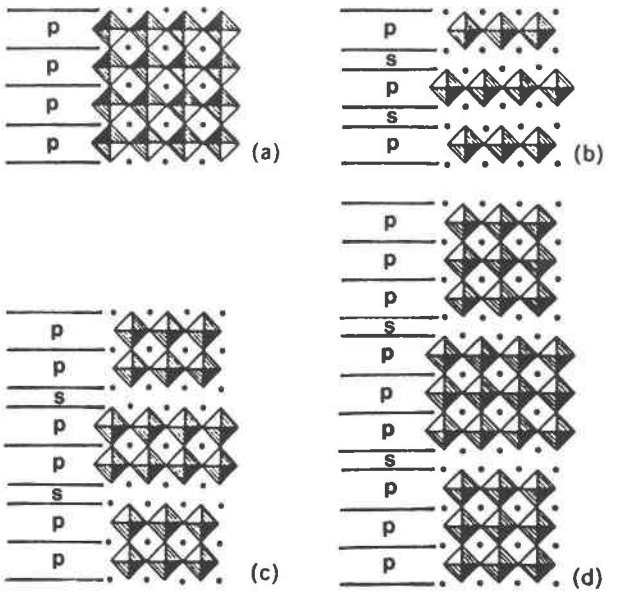

Fig. 6. Dilatational CS structures formed from the parent perovskite structure, showing that CS structures can be represented as polysomes. (**a**) The perovskite structure, sliced up into P slabs. (**b**) The polysome (PS), in which the CS-plane regions are defined as S slabs. (**c**), (**d**) The polysomes (PPS) and (PPPS), respectively. (After Tilley, 1980.)

ReO_3 and perovskite derivative structures: CS structures or polysomes?

A number of oxides, including WO_3 and mixed molybdenum tungsten, titanium tungsten, niobium tungsten, and tantalum tungsten oxides, crystallize with the ReO_3 structure type (Tilley, 1980). This structure consists of a three-dimensional framework of corner-sharing MO_6 octahedra. The perovskite structure is a simple stuffed derivative of ReO_3, obtained by stuffing cations into the cuboctahedral voids between the octahedra. These structures can be undistorted (the aristotype structure, see Megaw, 1973), or the octahedra can tilt to form a number of distortional variants that will not concern us here.

CS plane viewpoint. The ReO_3 or perovskite structure can be cut along a specially oriented surface and sheared such that one side of the crystal is moved relative to the other side by a vector that is not parallel to the plane of the cut, resulting in a crystallographic shear plane (i.e., the shearing vector possesses a component that does not lie within the plane). Figure 4 shows several ordered shear planes as they occur in the structure of the stoichiometric compound $W_{20}O_{58}$. Note that the WO_6 octahedra share edges, rather than corners, in the region of the shear and that the ratio of W to O is increased in this abnormal part of the structure. Such CS planes, which can occur in several orientations, are common as defects in reduced tungsten oxides, WO_{3-x}, as well as other oxides with this structure. These planar defects, rather than randomly distributed point defects such as vacancies or interstitials,

TABLE 1. Some polysomes observed in $(Na,Ca)_nNb_nO_{3n+2}$, $4 < n \leq 4.5$*

Polysome	Spacing, Å**	Na†	Ca	Nb	O
45	29.3	1	8	9	31
445	42.5	1	12	13	45
4445	55.7	1	16	17	59
44445	68.9	1	20	21	73
444445	82.1	1	24	25	87
444444444444444445	240.5	1	72	73	255
45445	71.8	2	20	22	76
454445	85.0	2	24	26	90
4454445	98.2	2	28	30	104
44544445	111.4	2	32	34	118
444544445	124.6	2	36	38	132
4545445	101.1	3	28	31	107
45445445445	156.8	4	44	48	166
4454454454445	183.2	4	52	56	194
44454445444544445	236.0	4	68	72	250
4445444454444544445	262.4	4	76	80	278
44454444544454444445	275.6	4	80	84	292
44544544544544545	241.8	6	68	74	256
4445445444544544545	268.2	6	76	82	284
444454445444445444544454445	360.6	6	104	110	382
444454445444454444544454445	373.8	6	108	114	396
44544544454444445444454444444444445	453.0	6	132	138	480
44545454545454545	247.6	8	68	76	262
454545454545454445	353.2	8	100	108	374
445444544544454454445444544454445	406.0	8	116	124	430
4545445454454454454454454445	385.4	10	108	118	408
445454454545445445445445445	385.4	10	108	118	408
444454545444544544445444445444544544454445	655.2	12	188	200	694

* Modified from Portier et al. (1975) and Tilley (1980).
** The length in Å of the sequence, equal to either d_{010} or $d_{010}/2$.
† Numbers refer to the number of atoms in the chemical formula.

are the dominant mechanism for accommodating appreciable nonstoichiometry in many ReO_3-type oxides, and they also can form in the perovskite structure type (Tilley, 1980). A high-resolution transmission electron microscopy (HRTEM) image of a shear plane in a reduced tungsten oxide crystal is shown in Figure 5.

In addition to occurring randomly, CS planes can order into periodic arrays to form discrete compounds, as suggested by Figure 4. An example of a system that exhibits periodic CS structures is the $(Na,Ca)_nNb_nO_{3n+2}$ ($4 < n \leq 4.5$) group of compounds, which can be derived from the perovskite structure by dilatational shearing operations (Portier et al., 1975). Numerous compounds can be formed by varying the numbers of perovskite layers between the CS planes, as shown schematically in Figure 6. A list of some of the ordered structures that have been observed is given in Table 1.

Polysomatic series viewpoint. Another way of viewing the structures in Figure 6 involves slicing up the structure into only two types of slabs, labeled P and S (for perovskite slab and sheared slab). The structures can then be represented as polysomes, and it can be said that they form a polysomatic series. The structures shown in Figures 6a–6d are simply (P), (PS), (PPS), and (PPPS), respectively. This example illustrates a general principle: any CS structure can also be represented as a polysomatic structure, simply by representing the parent structure with one type of slab and the regions containing the shear planes with another type of slab.

Not all polysomes, however, can be described as CS structures. Another large group of ReO_3-derivative structures, commonly referred to by solid-state chemists as the intergrowth tungsten bronzes, contains slabs of tungsten trioxide structure interleaved with slabs of the hexagonal tungsten bronze structure (Hussain and Kihlborg, 1976; Tilley, 1980). Two of these structures are shown in Figure 7, along with a HRTEM image of one of them. Obviously they can be described easily with the polysomatic model, but they cannot be derived by a simple periodic shearing of either of the two parent structures.

Which is better, CS or polysomatic representation? In the viewpoint of the author, the crystallographic shear and polysomatic models are equally valid, and each has its strong points, some of which are elaborated later in this paper.

The utility of the CS model is obvious for many oxide CS systems, where the shear planes typically form during reduction reactions. In such cases, the reaction mechanism by which the CS structure forms is, quite literally, shearing of the structure by the CS displacement vector. In some systems, the shear planes have even been observed as they form in situ in the transmission electron microscope (Iijima, 1975). The CS model is geometrically simple, it provides an adequate representation of the derivative structure, especially in structurally simple groups of compounds, and it can be used easily to determine the stoichiometries of the ordered structures.

The polysomatic model also describes simple CS struc-

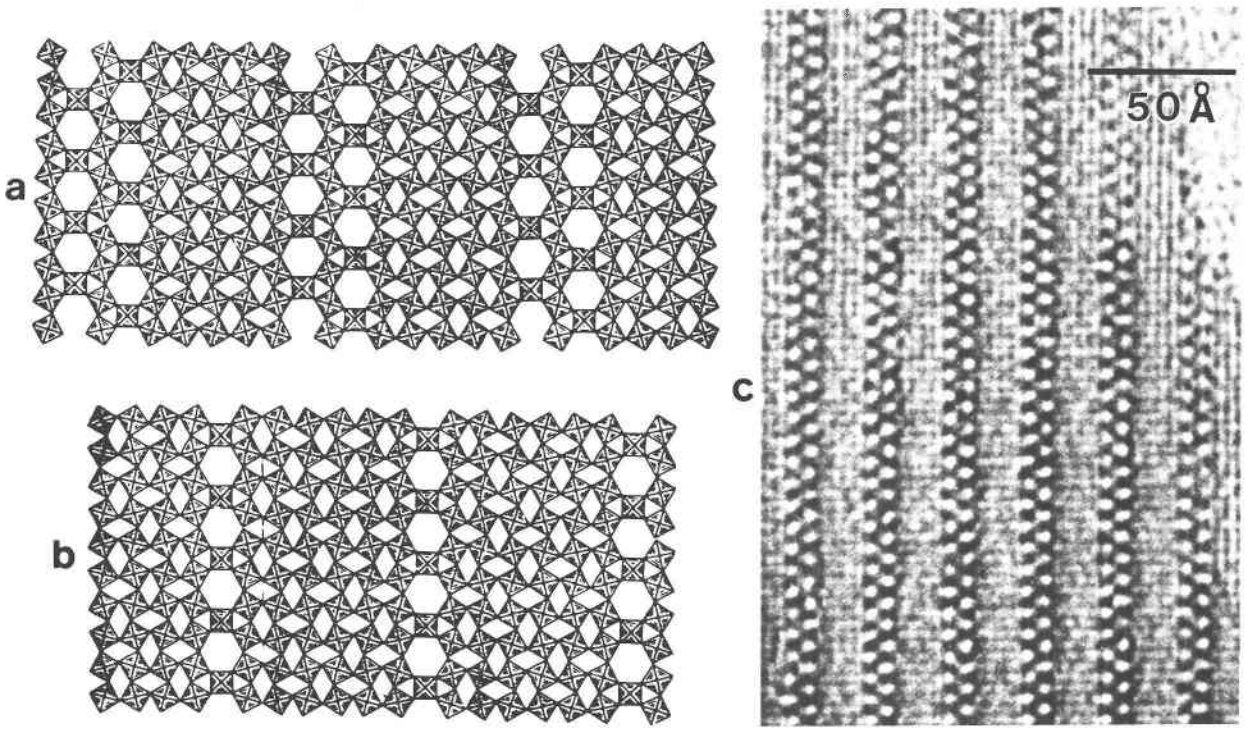

Fig. 7. Structures of two intergrowth potassium tungsten bronzes, K_xWO_3, with (**a**) double rows of the hexagonal tungsten bronze structure intergrown with slabs of ReO_3 structure and (**b**) single rows of the hexagonal tungsten bronze structure (from Tilley, 1987). (**c**) A HRTEM image of the structure shown in **a**, in which the double rows of prominent white dots correspond to the tunnels in the double rows of hexagonal tungsten bronze structure. (After Hussain and Kihlborg, 1976.)

tures adequately. However, it seems to be a more flexible model for describing a wide range of complex structures that include not only CS structures, but also intergrowth structures and those based on chemical twinning (see below). As we shall see, it can be used very simply to calculate the stoichiometry of both ordered and disordered structures, and it typically can predict details of polyhedral distortions and chemical partitioning trends that are not obvious from the CS model. Furthermore, CS structures commonly are produced directly by crystal growth or solid-state reactions that do not involve structural shear, and the mechanisms of some reactions can be understood better with the polysomatic model.

Whichever model is used to represent CS structures, it must be recognized that this structural principle encompasses a very wide range of important minerals and synthetic materials. As noted previously, in addition to the oxides based on the ReO_3 and perovskite structures, there are major CS systems derived from the rutile (Bursill and Hyde, 1972; Hyde, 1976) and Nb_2O_5 (Tilley, 1980) structures. Many structures, such as that of amphibole, that mineralogists know as polysomes also can be represented as CS structures (Chisholm, 1975). A final point again can be illustrated with the perovskite-based CS structures: some polysomatic series based on crystallographic shear operations are extremely complex. This is illustrated by Table 1, which lists only a fraction of the ordered structures that have been observed in the $(Na,Ca)NbO_{3+x}$ system. In order to simplify and comprehend such complex systems, it is essential to use some modular crystallographic model, and the one that is chosen is more a matter of taste and a function of the application at hand than a matter for debate.

Chemical twinning and polysomatism

As noted above, some modular structures can be represented by a chemical twinning model (Andersson and Hyde, 1974; Takéuchi, 1978; Tilley, 1987; Eyring, 1988). Although such structures occur in many nonmineral systems, there are numerous mineralogical examples, and we will enumerate a few of these.

Sulfosalts and oxysulfides. It has long been recognized that certain sulfides and sulfosalts form chemically and structurally coherent groups (e.g., Wuensch, 1974). One of the simplest of these is the PbS-Bi_2S_3 system. As shown by Takéuchi (1978), the galena structure can be twinned by reflection on (311), as shown in Figure 8a. When the structure of the twin boundary is relaxed, new crystallographic sites that can accommodate both Pb and Bi are formed, analogous to the way in which new types of sites are formed along the grain boundaries of metals (e.g., Frost et al., 1980). If the twinning is periodic, discrete minerals are formed; Figures 8b and 8c show the structures of heyrovskyite and lillianite (Takéuchi, 1978), which

are produced by different spacings between the twin planes. As shown, these structures can be spliced up into two kinds of slabs, labeled G and B, and their treatment as polysomes is hence obvious; the structures shown here are of (G_7B) and (G_4B). The chemical composition varies as the ratio of the two types of slabs changes. The clearest difference between this example and the polysomes that can be represented as CS structures is that the G slabs occur in two orientations, rather than in one. Additional examples of sulfosalts that can be represented as polysomes and of sulfosalt polysomatic series are presented in an extensive review by Makovicky (1989).

Other examples of S-bearing polysomes occur in the schafarzikite polysomatic series. Whereas schafarzikite is an iron and antimony oxide, it contains structural slabs that can intergrow with S-bearing slabs to form the oxysulfide polysomes versiliaite and apuanite (Ferraris et al., 1986).

Oxyborates. As shown by the structure determinations of Moore and Araki (1974) and Takéuchi et al. (1978), certain metal oxyborates represented by the formula $Me_3O_2[BO_3]$, Me = Mg, Fe, Al, Mn . . . , can be represented as chemical twin structures (Takéuchi, 1978). Consisting of structurally similar slabs that are periodically twinned to produce an anomalous structure at the twin planes, these oxyborates are analogous to the sulfosalts described in the last section. The frequency of the twin planes controls both the crystal structure and the amount of Mn^{3+} in both natural and synthetic ludwigite, orthopinakiolite, pinakiolite, and takéuchiite. Furthermore, mistakes in the periodicity of the twin planes lead to structural disorder and chemical variations in all of these minerals (Bovin and O'Keeffe, 1981; Bovin et al., 1981a, 1981b).

Enstatite-IV. Silicates of the $Mg_2Si_2O_6$-$LiScSi_2O_6$ solid-solution series crystallize either with the clinopyroxene structure or with one of several structures having discontinuous silicate chains (Takéuchi, 1978). In the latter structures, termed the enstatite-IV series, the chain segments possess 8, 9, or 10 tetrahedra, and the twin-related segments are separated by a slab of anomalous structure (Fig. 9). If the wide clinopyroxene slabs shown in Figure 9 are cut into narrower slabs that are one tetrahedron wide, and these slabs are interleaved with a slab of the chain-interrupting structure, then the structures of the enstatite-IV series can be represented as a polysomatic series with pyroxene as one end-member (Thompson, 1978). This is only one of at least three polysomatic series that can be formed with pyroxene, since the biopyriboles and the pyroxenoids also have pyroxenes as end-member structures.

Humite group. Thompson (1978) showed clearly that the humite group can be represented as a polysomatic series constructed from slabs of olivine and norbergite structure. Thompson pointed out that two different orientations of the olivine slab, O_L and O_R, and two orientations of the norbergite slab, N_L and N_R, are required to represent all of the structures in the polysomatic series

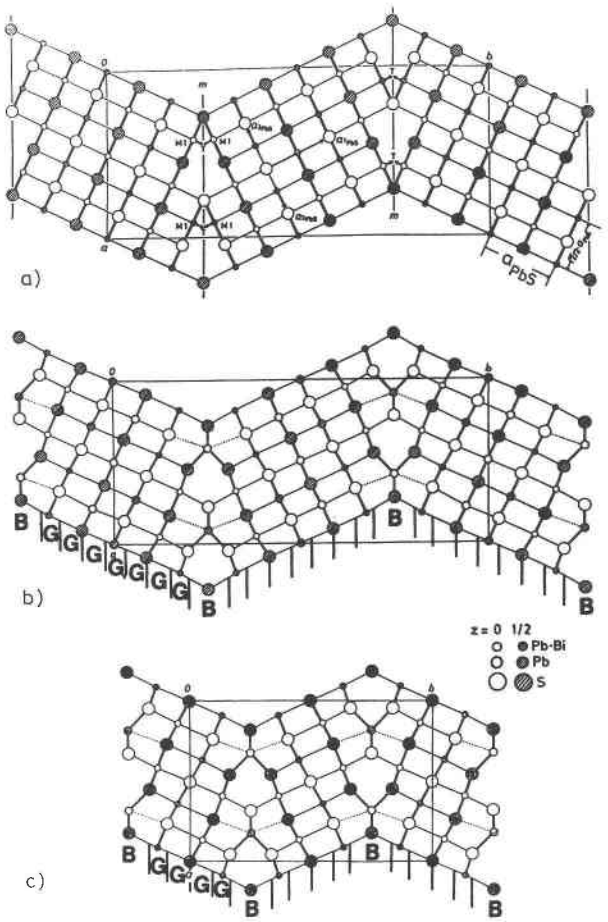

Fig. 8. Chemical twinning structures based on the galena structure. (**a**) The structure of galena artificially twinned on the (311) planes. (**b**) The structure of heyrovskyite, showing how the structure in the twin planes has relaxed relative to that of the artificially twinned structure. Slabs of galena structure, G, and the twin boundary structure, B, are indicated to show how this CT structure can also be represented as the polysome (G_7B). (**c**) The structure of lillianite, shown as the polysome (G_4B). (After Takéuchi, 1978.)

norbergite-chondrodite-humite-clinohumite-olivine; the positions of the octahedrally coordinated cations in the series are shown in Figure 10. In fact, the L and R slabs of Thompson (1978) are related by the (001) mirrors in the olivine and norbergite structures, and thus it is apparent that these polysomes also can be described as chemical twinning structures (O'Keeffe and Hyde, 1985). Note, however, that the (001) mirrors are present as symmetry elements in not only the two parent structures, but also in humite. As such, these mirrors by definition cannot be true twinning operations of the overall structures, pointing out the potential confusion arising from the term "chemical twinning" noted earlier. In an alternative description of the humite group structures, O'Keeffe and Hyde (1985) focused on the cation packing, noting that

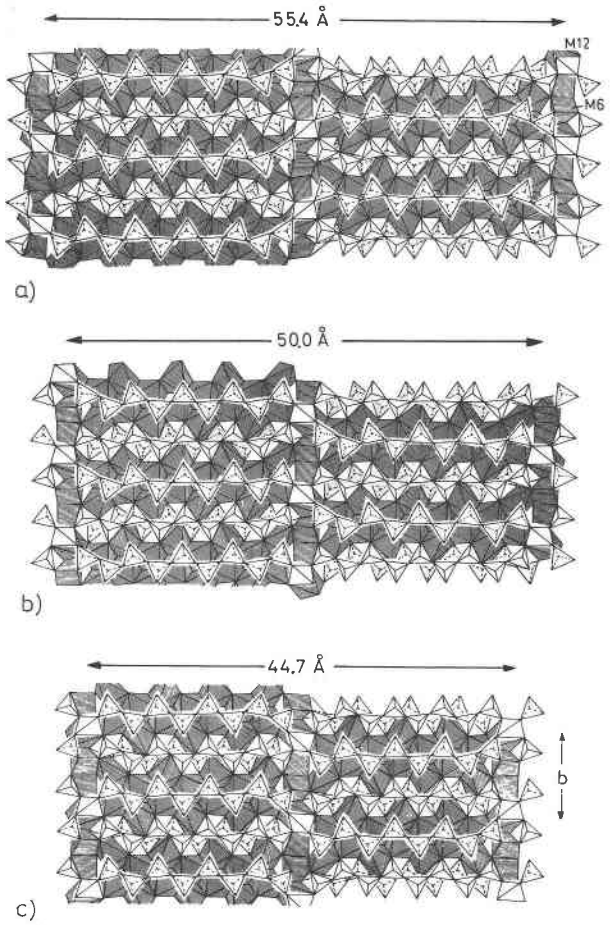

Fig. 9. The enstatite-IV structures, showing how the number of tetrahedra in the interrupted chains varies from (a) 10 to (b) 9 to (c) 8. (From Takéuchi, 1978.)

this description is simpler than the classical description based on O closest packing.

Polysomatic series based on chain/sheet structures

A number of polysomatic series possess as their two end-members a chain structure and a sheet structure (e.g., the barium silicates: Liebau, 1985, ch. 10). In general, the intermediate polysomes in such a series are also chain structures, but the widths (or multiplicities) of the chains are greater than in the end-member chain structure. Two such silicate series are described briefly in this section, and a similar case in the manganese oxides is covered later.

Biopyriboles. Due to Thompson's seminal 1978 paper on polysomatic series, as well as their petrologic importance, the biopyriboles are probably the best-known group of polysomatic minerals. The biopyriboles include the pyroxenes, amphiboles, and 2:1 sheet silicates, which have been extensively reviewed previously (Prewitt, 1980; Veblen, 1981a; Veblen and Ribbe, 1982; Bailey, 1984, 1988). In some cases, the term biopyribole has been used incorrectly to refer only to those relatively rare biopyribole structures containing triple or wider chains (Veblen, 1981b). The term as defined by Johannsen (1911) and Thompson (1978), however, clearly includes pyroxenes, amphiboles, micas, talc, etc., in addition to the more recently discovered wide-chain members of the group.

Although they are well known, the idealized structures of clinoamphibole (double-chain silicate) and clinojimthompsonite (triple-chain silicate) are shown in Figure 11 because of the importance of the pyroxene–2:1 sheet silicate polysomatic series. The illustrated structures can be thought of as interleaved slabs of pyroxene (P) and mica or talc (M) in the sequences (MP) and (MMP). The biopyriboles will be used as examples later in this paper, but note here that they constitute but one of several polysomatic systems that contain both chain and sheet structures.

Carlosturanite. The recently discovered mineral carlosturanite is a chain-silicate derivative of the 1:1 sheet silicate lizardite, one of the forms of serpentine (Mellini et al., 1985; Ferraris et al., 1986); it appears likely that this fine-grained mineral is commonly mistaken for serpentine. The structure of carlosturanite can be represented as a polysomatic mixture of lizardite slabs (S) and another type of slab (X) in which vacancies replace Si atoms in a lizardite-like structure. Carlosturanite is then

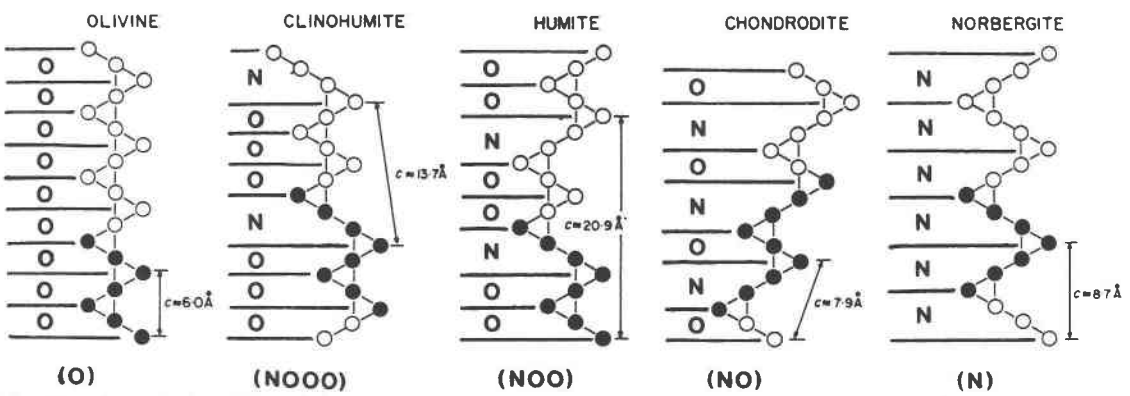

Fig. 10. The zigzag chains of the olivine-humite group polysomatic series; the circles represent the positions of the octahedrally coordinated cations. The series can be represented as mixtures of olivine "O" slabs and norbergite "N" slabs. Norbergite = (N), chondrodite = (NO), humite = (NOO), clinohumite = (NOOO), and olivine = (O). (Modified from Papike and Cameron, 1976.)

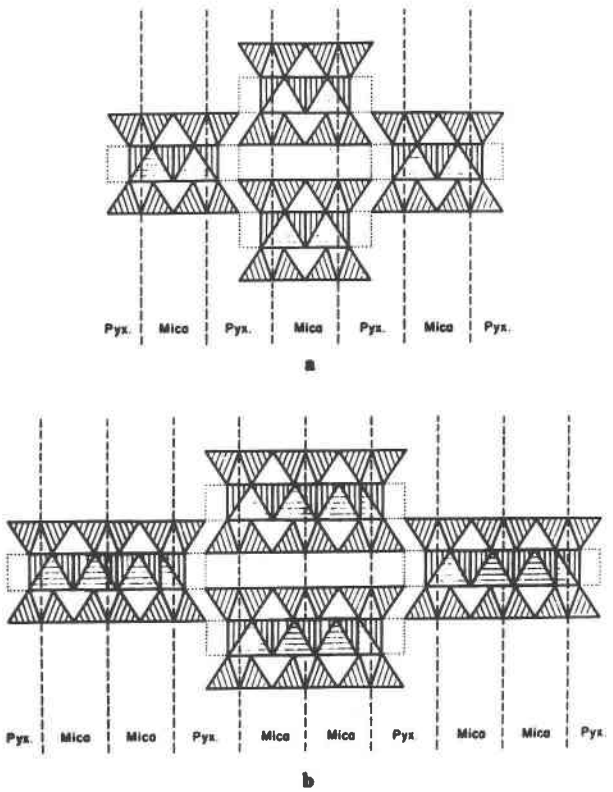

Fig. 11. The idealized structures of (**a**) clinoamphibole and (**b**) clinojimthompsonite, showing how pyriboles can be regarded as P slabs of pyroxene structure and M slabs of mica or talc. Amphibole is the polysome (MP), whereas jimthompsonite and clinojimthompsonite are (MMP). (From Thompson, 1978, and Veblen, 1981b.)

the polysome (SSSSSX), or (S_5X), as shown in Figure 12a. Several other polysomes, such as (S_4X) (Fig. 12b) have been observed as defects within carlosturanite.

Like the biopyribole polysomatic series, the series containing carlosturanite possesses a sheet silicate (lizardite) as one of the end-member structures. Although the X slabs in Figure 12 produce a sorosilicate when mated, a redefinition of these slabs to include half of an S slab on each side would yield modules that could be combined to form a chain silicate. In recognition of the chain and sheet structures within this series, it has been named the inophite polysomatic series (Mellini et al., 1985; Ferraris et al., 1986).

Antigorite: polysomes with three structurally distinct modules

The serpentine mineral antigorite is one of a large number of minerals with corrugated silicate sheets, in which the apical O atoms of the tetrahedra can point to either one side of the sheet or the other (Liebau, 1985, ch. 10). As shown by Spinnler (1985), Livi and Veblen (1987a), and Mellini et al. (1987), the antigorite structure of Kunze (1961) can be represented as a polysomatic series based on three types of slabs: (1) a lizardite slab, (2) a slab in which the direction of the apical O atoms switches and

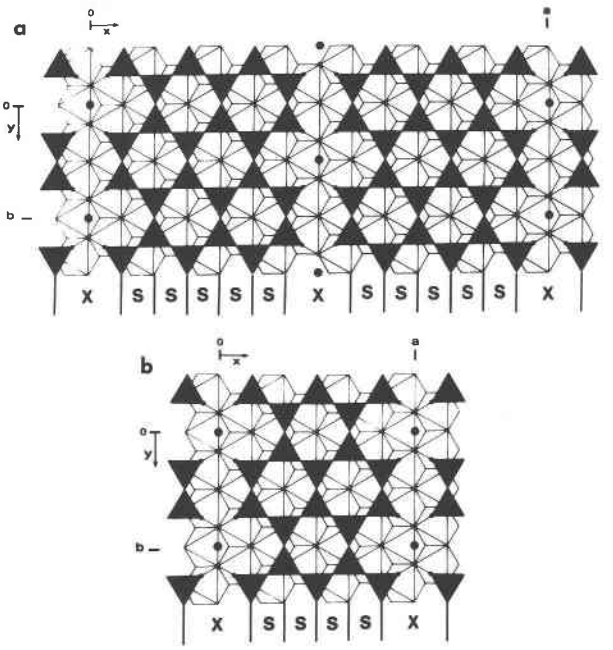

Fig. 12. (**a**) The carlosturanite structure, which can be represented as the (S_5X) polysome constructed from modules of the serpentine mineral lizardite (S) and a related slab containing tetrahedral vacancies (X). (**b**) The (S_4X) polysome, which is one of several types of defects that occur intergrown with carlosturanite. (After Mellini et al., 1985.)

that contains six-membered silicate rings, and (3) a similar slab with eight- and four-membered rings. Each unit cell contains a number of lizardite slabs but only one six-membered reversal slab and one eight-membered slab (Fig. 13). Thus, if the antigorite structure of Kunze (1961) is correct, this mineral presents a rather unusual case in which a polysome contains three structurally and chem-

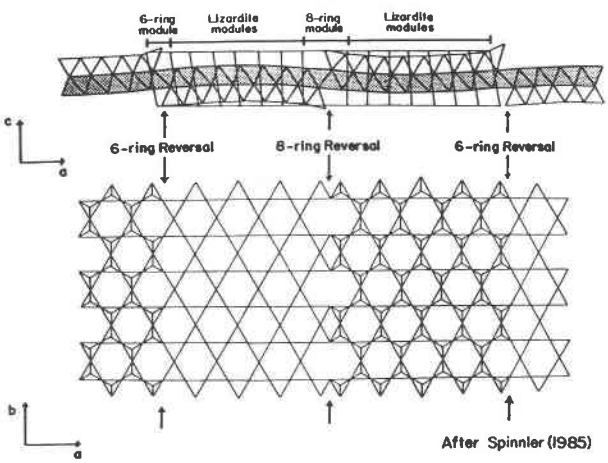

Fig. 13. Two views showing how the antigorite structure(s) can be represented as a polysomatic series constructed of lizardite modules and two types of sheet reversal slabs (after Spinnler, 1985). The structure, chemical composition, and *a* unit-cell parameter vary as the number of lizardite slabs between reversal slabs changes. (From Livi and Veblen, 1987a.)

TABLE 2. Unit-cell parameters and metal atom coordinates for johannsenite and the pyroxmangite P region transformed into a pyroxenelike unit cell

		Pyroxmangite*	Johannsenite**
		Unit cell	
a		10.05 Å	9.98 Å
b		8.88 Å	9.16 Å
c		5.58 Å	5.29 Å
α		89.82°	90°
β		110.02°	105.48°
γ		89.78°	90
		Metal positions	
M2/M1†	*x*	0.000	0
	y	0.104	0.095
	z	0.745	¾
M2/M1	*x*	0.000	0
	y	0.896	0.905
	z	0.255	¼
M3/M1	*x*	0.500	½
	y	0.604	0.595
	z	0.745	¾
M3/M1	*x*	0.500	½
	y	0.396	0.405
	z	0.255	¼
M5/M2	*x*	0.000	0
	y	0.726	0.698
	z	0.759	¾
M5/M2	*x*	0.000	0
	y	0.274	0.302
	z	0.241	¼
M5/M2	*x*	0.500	½
	y	0.226	0.198
	z	0.759	¾
M4/M2	*x*	0.512	½
	y	0.782	0.802
	z	0.248	¼
Si5/Si	*x*	0.789	0.787
	y	0.409	0.408
	z	0.791	0.736
Si6/Si	*x*	0.789	0.787
	y	0.578	0.592
	z	0.306	0.236
Si5/Si	*x*	0.289	0.287
	y	0.909	0.908
	z	0.791	0.736
Si4/Si	*x*	0.292	0.287
	y	0.085	0.092
	z	0.272	0.236
Si3/Si	*x*	0.210	0.213
	y	0.588	0.592
	z	0.244	0.264
Si4/Si	*x*	0.208	0.213
	y	0.415	0.408
	z	0.728	0.764
Si3/Si	*x*	0.710	0.713
	y	0.088	0.092
	z	0.244	0.264
Si2/Si	*x*	0.709	0.713
	y	0.918	0.908
	z	0.769	0.764

* Pyroxmangite structural data from Ohashi and Finger (1975).
** Johannsenite structural data from Freed and Peacor (1967).
† Atomic site nomenclature is given as pyroxmangite-johannsenite.

ically distinct types of slab. The number of lizardite slabs in each unit cell can be varied, producing a polysomatic series of discrete antigorite structures having different *a* unit-cell parameters and different compositions, in some cases within the same nominal crystal. Ferraris et al. (1986) presented a simplified model in which slabs (2) and (3) are similar, but very different beam damage rates for the two slabs in HRTEM studies (Spinnler, 1985; Livi and Veblen, 1987a) suggest that they are truly distinct.

Pyroxenoids: how close is the slab structure in polysomes to that of the parent structures?

It was suggested by Koto et al. (1976) that the pyroxenoid structures can be represented as mixtures of the clinopyroxene and wollastonite structures. Thompson (1978) noted that wollastonite, rhodonite, pyroxmangite, ferrosilite-III, and clinopyroxene form the polysomatic series (W), (WP), (WPP), (WPPP), (P), and this device subsequently has been used by numerous authors working with pyroxenoids (e.g., Czank and Liebau, 1980; Veblen, 1985a; Pinckney and Burnham, 1988). Taking a different view, Angel (1986b) asserted that the P slabs in pyroxenoids do not possess the pyroxene structure and that, when transformed into a pyroxenoidlike unit cell, slabs of pyroxene do not even have the *C*-centered lattice necessary for them to mate with the W slabs. The relationship between pyroxene and pyroxenoid P slabs thus requires resolution and also permits us to ask how similar a slab in a polysome is to the same type of slab residing within the parent structure. The detailed unit-cell transformations that support the discussion below are given in Appendix 1.[1]

Angel (1986b) transformed the **b** axis of clinopyroxene to $\mathbf{b}' = \mathbf{b} - \mathbf{c}$, asserting that $\mathbf{b}'$ is analogous to **b** of the pyroxenoids. The resulting unit-cell transformation produces a body-centered lattice, and Angel then concluded that such a unit cell is incompatible with the W slabs of pyroxenoids. Several authors have noted, however, that clinopyroxenes and pyroxenoids intergrow on $\{11\bar{1}\}$ of pyroxene (Czank and Simons, 1983; Ried, 1984; Angel et al., 1984; Angel, 1986b; Veblen, 1985a), indicating that the **a** axis also must be transformed to place the clinopyroxene structure in a pyroxenoidlike unit cell. The resulting transformation of basis vectors (Appendix 1) leaves the pyroxene *C* centered and hence compatible with the W slabs, as also noted by Angel and Burnham (1991).

When part of the P-slab region of a pyroxenoid is transformed into a clinopyroxenelike unit cell, it is clear that it is isostructural with pyroxene (Table 2). Although there are subtle differences in the structures, the two unit cells are very close, the angles α and γ in the transformed unit cell of pyroxmangite are near the ideal 90° for clinopyroxene, and the fractional coordinates for pyroxene and pyroxenoid are similar.

The relationship between back-to-back chains in the pyroxenelike part of pyroxmangite and in johannsenite is shown in Figure 14. Although there is a slight shift between the chains in pyroxmangite relative to those of johannsenite, as reflected by the larger angle β in the transformed pyroxenoid cell of Table 2, the two structures are

[1] A copy of Appendix 1 may be ordered as Document AM-91-458 from the Business Office, Mineralogical Society of America, 1130 Seventeenth Street NW, Washington, DC 20036, U.S.A. Please remit $5.00 in advance for the microfiche.

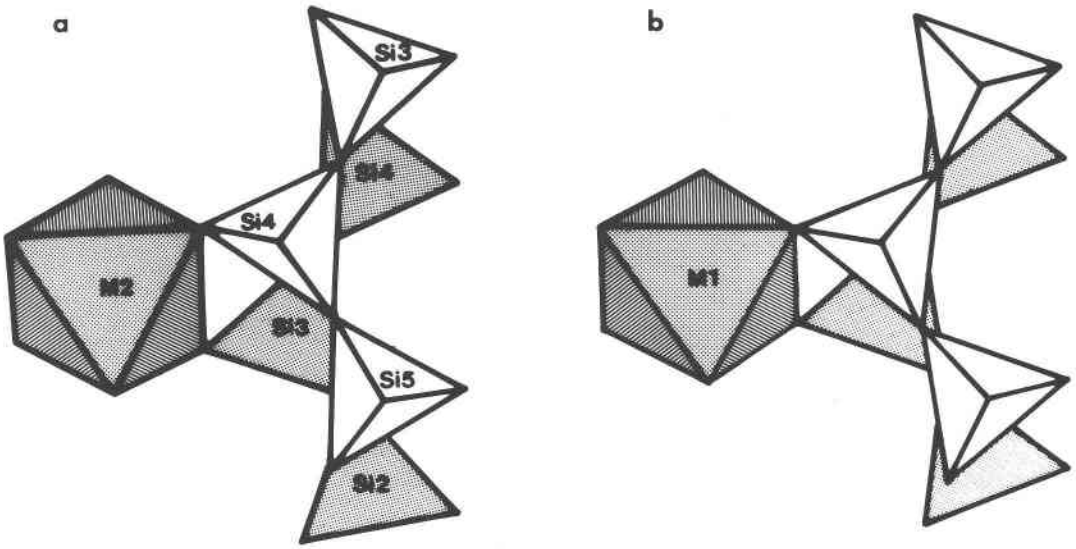

Fig. 14. The relationship between back-to-back silicate chains in (**a**) the pyroxenoid pyroxmangite and (**b**) the clinopyroxene johannsenite. The structures are very similar and are largely controlled by the coordination requirements of the regular octahedral sites. The back-to-back silicate chains in the pyroxenoid are not offset by $c/2$ relative to those in the clinopyroxene.

remarkably similar. This striking similarity is also shown by Angel and Burnham (1991), who compared synthetic $MnSiO_3$ clinopyroxene with a structure constructed from pyroxmangite P slabs. Certainly the back-to-back silicate chains are not offset by **c**/2 in pyroxene relative to pyroxenoid, as suggested by Angel (1986b, Fig. 2). The offsets between back-to-back silicate chains in pyroxenoids and clinopyroxenes are similar because they are constrained by the linkage between the chains through the regular octahedra of the octahedral strips (i.e., M1 in pyroxene nomenclature).

Based on Table 2, Figure 14, and the work of Angel and Burnham (1991), it can be concluded that the P slabs in pyroxenoids are structurally very similar to clinopyroxene. Pinckney and Burnham (1988), in a detailed analysis of the polyhedral distortions and interatomic distances in rhodonite and pyroxmangite, pointed out that the degree of distortion away from the pyroxene structure is slight at the boundaries between P slabs and is most pronounced in the regions where the P slabs must mate with the W slabs. Similarly, variations in the chemistry of metal sites lead to minor structural variations, as can be seen in Figure 14 and the diagrams of Angel and Burnham (1991). As shown by Pinckney and Burnham (1988), though, even in the most distorted parts of the structure, the P and W parts of the pyroxenoids are recognizable as pyroxene-like and wollastonite-like. This is also the case for other polysomatic systems, such as the biopyriboles. It seems likely that if the structural distortions required for mating the two types of slab in a polysome were too great, then the energy of the resulting structure would be too great for it to form. It would be interesting to test this notion by calculating the structure energies of hypothetical polysomatic structures that are highly distorted. As noted by Thompson (1981a), many conceivable polysome compositions do not form in the biopyribole system, simply because the misfit between the M and P slabs is too great.

Sheet silicates: use of polysomatism for constructing computer structure models

Thompson (1978) demonstrated that many of the rock-forming sheet silicates can be represented as polysomes constructed from a few distinct modules. As in the case of the humite group, these modules commonly occur in more than one orientation, and the sheet silicates therefore could be thought of as chemical twinning structures if so desired. More interesting to mineralogists is that disordered sheet silicates can contain more than two types of polysomatic (001) slab (i.e., parallel to the layers), just as antigorite contains three types of (100) slabs (i.e., cutting across the layers).

Perhaps more than any other rock-forming mineral group, the sheet silicates are prone to structural disorder, largely related to aperiodicity in layer stacking sequences and the mixing of incorrect layers into many of the structures. One of the most powerful methods for studying such disorder is HRTEM, but accurate interpretation of the electron microscopy experiments requires the comparison of experimental images with images simulated by computer (e.g., O'Keefe, 1984; Self and O'Keefe, 1988). Such computer simulations require as input a model of the structure to be simulated; this model consists primarily of atomic coordinates, unit-cell parameters, and space-group information. For the simulation of crystal defects and structurally disordered materials, artificially large unit cells must be used (see, for example, Veblen,

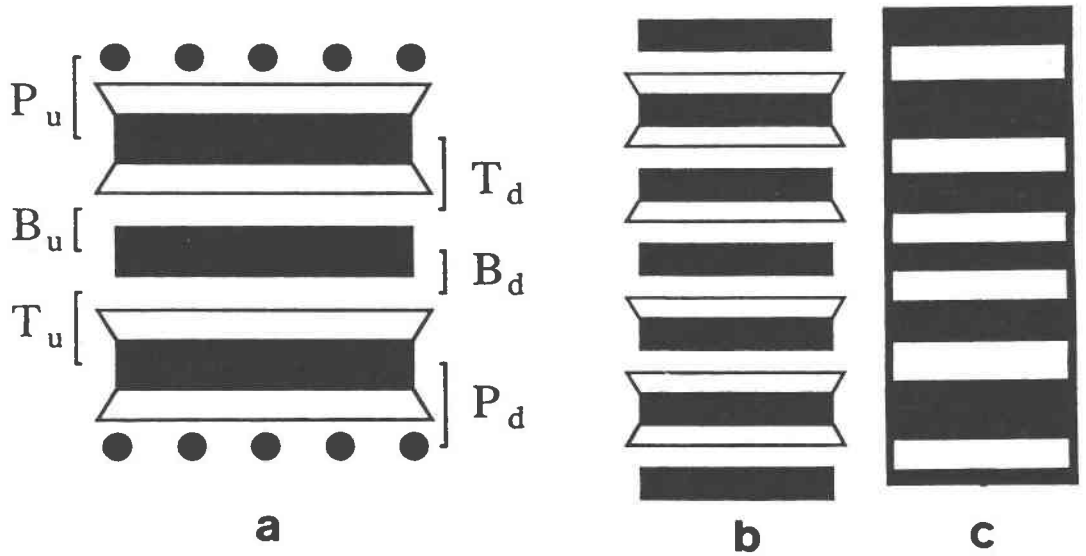

Fig. 15. (**a**) Polysomatic sheet silicate modules after Thompson (1978), which can be used to generate structural models of both simple and mixed-layer sheet silicates and hydroxides. P_u,P_d = twin-related phlogopite modules; T_u,T_d = talc modules; B_u,B_d = brucite modules. (**b**) An example of a model mixed-layer structure generated by combining the modules in **a**. This structure, which contains 1:1 and 2:1 layers and hydroxide sheets, contains nearly 1000 atoms per unit cell. (**c**) A simulated HRTEM image at Scherzer focus generated from the model structure in **b**, showing that the layers of different thicknesses can be imaged (but only under the most ideal of observing conditions). (From Guthrie and Veblen, 1990.)

1985b), and the resulting structural models therefore may contain many hundreds or even thousands of atoms.

The recognition that a structure is polysomatic can greatly simplify the construction of a structural model, if the aperiodic aspect of the structure is related to disorder in the placing of the polysomatic slabs. (Luckily, as discussed below, it is polysomatic structures that tend to show the greatest degrees of structural disorder among the rock-forming minerals.) For polysomes, a structural model can be assembled with a computer by assuming that the atomic coordinates and site occupancies in all slabs of the same type are identical. Once the structure of each slab type has been introduced as input, the desired structure can be assembled by adding appropriate translation vectors and scaling the atomic coordinates for the size of the composite unit cell.

The sheet silicates present a simple example of such exploitation of polysomatism. The structural modules defined by Thompson (1978) are shown in Figure 15a. By assembling these in the desired order, all of the atomic coordinates and site occupancies can be generated easily by computer for any structure composed of these slabs, such as the one shown in Figure 15b. Figure 15c illustrates a computer simulation of a HRTEM image for this structure. For the particular imaging conditions of this simulation, the image strongly resembles the structure, but it can be shown that for other conditions, incorrect identification of the layers in the structure would result from intuitive interpretation. Guthrie and Veblen (1990) employed extensive simulations of computer-generated models of sheet silicates to outline the HRTEM imaging conditions appropriate for the observation of structural disorder in a wide range of rock-forming sheet silicates, and Guthrie and Veblen (1989) and Veblen et al. (1990) used similar methods to facilitate the imaging and image interpretation for mixed-layer illite/smectite clays. Although the simple example given here is for a one-dimensional imaging problem, analogous methods have been used to create structural models for more complex defects. An example is the simulation of complex HRTEM images of defects in biopyriboles by assembling the M and P modules in appropriate arrays (e.g., Veblen and Buseck, 1980).

Tunnel and sheet manganese oxides: two-dimensional polysomatism and block structures

Although the manganese oxide minerals typically occur as extremely fine-grained polycrystalline masses and mixtures, there has been much recent progress in understanding their crystal chemistry. Many of the advances have come through the application of HRTEM methods (Turner and Buseck, 1979, 1981, 1983), as well as careful single-crystal X-ray diffraction experiments (Post et al., 1982; Post and Appleman, 1988; Turner and Post, 1988) and Rietveld refinement of powder X-ray data (Post and Bish, 1988, 1989; Post and Veblen, 1990). Nonetheless, there is still debate over some of the structures and terminology (e.g., Giovanoli, 1985; Burns et al., 1985). Like the biopyriboles, the manganese oxides that contain predominantly Mn^{4+} occur either with chains (the tunnel

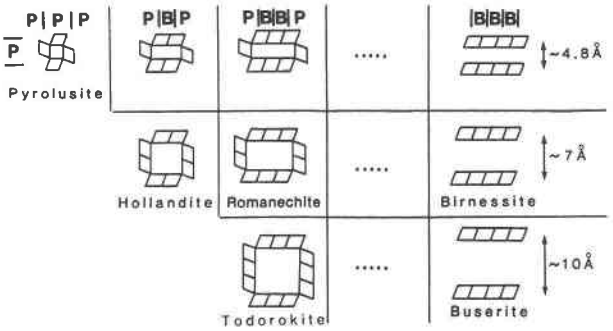

Fig. 16. Idealized structures of some of the chain and sheet manganates (after Buseck and Veblen, 1988, following Turner and Buseck, 1979, 1981, 1983, and the classification scheme of S. Turner, personal communication). The first row consists of the polysomes pyrolusite (P) with 1 × 1 tunnels, (PB) with 2 × 1 tunnels, (PBB) with 3 × 1 tunnels, and a collapsed birnessite-like structure (B) which is ∞ × 1. These structures then serve as the parent structures for polysomatic series in the vertical direction, which give rise to the 2 × 2 hollandite, 3 × 1 romanechite, 3 × 3 todorokite, etc. This two-dimensional set of polysomatic series is analogous to block structures (see text and Fig. 17).

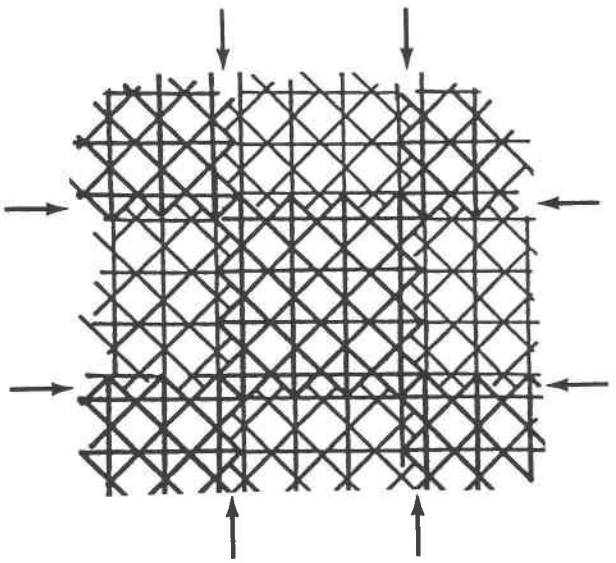

Fig. 17. The structure of M-Nb_2O_5, which is one of many block structures in the niobium and niobium-titanium oxide system. This 3 × 3 structure can be thought of as two intersecting sets of periodic CS planes (arrows), or as a two-dimensional set of polysomatic series. (After Anderson, 1972.)

structures) or with sheets (the phyllomanganates). Also like the biopyriboles, the tunnel structures can contain chains of variable width, and the sheet structures, like smectites, can exhibit variable occupancy of interlayer sites, layer swelling and collapse, and rapid cation exchange (Golden et al., 1986).

Figure 16 shows the basic building blocks of the predominantly tetravalent manganese oxides. The first row shows some 1 × N structures with N values of 1, 2, 3, and ∞, sliced up into polysomatic slabs (the numbers refer to the widths of the manganate chains). The 1 × 1 structure (pyrolusite) is (P), the 1 × 2 structure is (PB), the 1 × 3 structure is (PBB), and the sheet structure (similar to a collapsed birnessite) is (B). What differentiates this structural system from the other polysomatic series we have examined is that the structures in the first row can themselves be used as base structures to form the other structures shown in Figure 16 by forming polysomes with slabs in an orientation approximately normal to that of the first set of slabs, thus forming the hollandite, romanechite, and ideal todorokite structures.

Several points can be made about these structures. First, all of these polysomes can have the same chemical composition, MnO_2, but in fact the structures with the larger tunnels commonly exhibit a least partial occupancy of the tunnels by various cations, with charge compensation arising from reduction of part of the Mn. These tunnel cations are analogous to the interlayer cations of the sheet structures and can be thought of as similar to the A-site cations of amphiboles and wide-chain biopyriboles. In cases where such occupancy is appreciable, separate mineral names have been applied, such as cryptomelane ($K_{1-2}Mn_8O_{16}\cdot nH_2O$) and coronadite ($Pb_{1-2}Mn_8O_{16}\cdot nH_2O$). The ratios of the various structural slabs therefore appear to be correlated to chemical variations, as is typical for polysomatic series.

The polysomatic model is a somewhat awkward device for describing the structures of these manganese oxides, since the polysomatic slabs cross each other. This system can be thought of as a primary polysomatic series (the first row of Fig. 16) from which parasitic polysomatic series are derived (the columns of Fig. 16). In fact, this type of structural relationship is well known in the field of solid-state chemistry, where structures having intersecting CS planes are called "block structures." An example of such a block structure in the compound Nb_2O_5 is shown in Figure 17. A very large number of similar block structures have been recognized (Anderson, 1972), and they could be described by the same sort of two-dimensional systems of polysomatic series as one can use for the manganese oxides.

Applications of the polysomatic model

Structural disorder

Since the initial publication of the polysomatic model (Thompson, 1970, 1978), it has become clear that one of its most important applications is in understanding structural disorder in minerals and other compounds. Indeed, structures that can be constructed from layers are inherently prone to planar defects. In polytypic structures, mistakes in the stacking sequence of layers are common; it is very unusual in TEM investigations of sheet silicates, for example, to find crystals that are entirely without stacking faults, and stacking disorder is rampant in many sheet silicates.

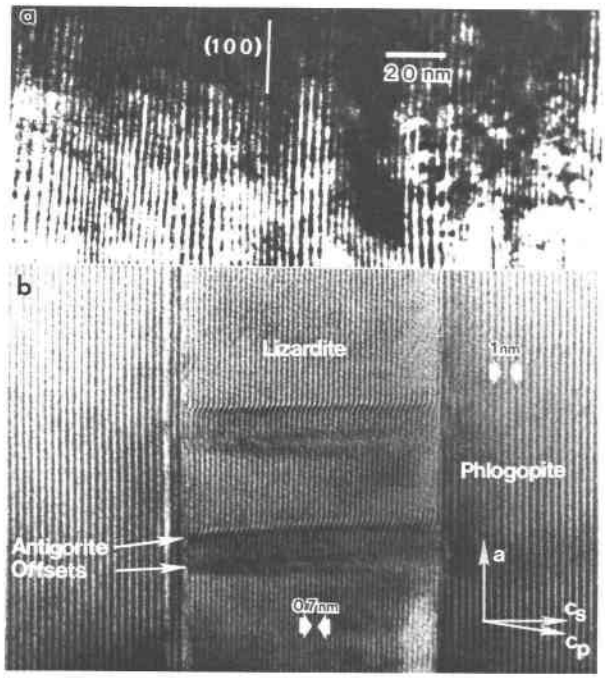

Fig. 18. (**a**) HRTEM image of an antigorite "crystal." The (100) fringes show that there is considerable variation in the modulation period of the structure, as a result of variations in the numbers of lizardite modules between the reversal slabs of the structure (see Fig. 13). (After Spinnler, 1985.) (**b**) A lamella of serpentine in phlogopite. The serpentine is a polysomatic intergrowth consisting primarily of the planar structure lizardite, with two pairs of nonperiodic offsets characteristic of the antigorite structure. (From Livi and Veblen, 1987a.)

Likewise, in polysomatic structures, an obvious way to create a planar defect is to leave out a polysomatic slab from the normal, periodic sequence, or to insert an extra slab. Such defects are important not only for energetic considerations, but also because they alter the stoichiometry of a crystal. If polysomatic defects are abundant, the deviations can cause a crystal to have a stoichiometry substantially different from that of its nominal structural formula. In fact, defects based on the principle of missing or extra polysomatic slabs have been recognized in virtually every mineral system that can be described by the polysomatic model, though the frequency of their occurrence is highly variable from system to system. In the extreme case, crystals with apparently random sequences of slabs can form. It is not my intention to review thoroughly the extensive literature on such structural disorder. Instead, I offer the following examples and a few references to the types of polysomatic structural disorder that have been observed.

Perhaps the best-known mineralogical polysomatic defects occur in the biopyribole system. Here an M slab inserted into pyroxene (P) can produce an isolated slab of amphibole structure MP; a missing M slab in amphibole can produce a slab of pyroxene chains; an extra M slab in amphibole (MP) can produce a triple-chain defect MMP; or a string of extra M slabs can produce a talc-like or mica-like zone in either pyroxene or amphibole. In fact, the types of polysomatic defects that have been observed in biopyriboles could be enumerated ad nauseum (see, for example, Chisholm, 1973; Hutchison et al., 1975; Veblen et al., 1977; Veblen and Buseck, 1979, 1980, 1981; Nakajima and Ribbe, 1980, 1981; Maresch and Czank, 1983, 1988; review by Veblen, 1981b). It is worth noting that the frequency of such defects depends strongly on chemical composition and paragenesis. For example, ferromagnesian amphiboles seem to be much more susceptible to extreme disorder of this type than calcic and alkali amphiboles.

Structural disorder is common in the families of compounds described in the section "ReO_3 and perovskite derivative structures," where the spacing between CS planes can vary from perfectly ordered to completely random (see reviews by Anderson, 1972; Tilley, 1980; Eyring, 1988). Polysomatic disorder also occurs in the sulfosalts and oxyborates described in the section on chemical twinning (Tilley, 1987; Eyring, 1988; Bovin and O'Keeffe, 1981; Bovin et al., 1981a). A wide range of polysomatic defects and intergrowths have been observed in at least three polysomatic series related to the olivine structure: the humite group (Müller and Wenk, 1978; White and Hyde, 1982a, 1982b), the related Mn silicate leucophoenicite (White and Hyde, 1983), and laihunite (Kitamura et al., 1984), as well as intergrowths of magnesian olivine and laihunite (Banfield et al., 1990).

In polysomes based on sheet silicates, polysomatic disorder has been observed in carlosturanite (Mellini et al., 1985). In antigorite, variations in the numbers of lizardite slabs between the reversal slabs can produce notable variations in the *a* unit-cell parameter (Spinnler, 1985; Mellini et al., 1987), as seen in Figure 18a. Disordered pairs of antigorite reversals also have been observed in lizardite, as shown in Figure 18b (Livi and Veblen, 1987a). The form of polysomatic order-disorder called mixed layering is well known in clay minerals, and it is not uncommon in rock-forming trioctahedral micas, chlorites, talc, etc. (e.g., Reynolds, 1980, 1988; Veblen, 1983; Maresch et al., 1985; Olives Baños, 1985; Amouric et al., 1988; Banfield et al., 1989).

Disorder in the sequence of P and W slabs occurs in both synthetic and natural pyroxenoids, and isolated slabs of pyroxenoid can be found in some pyroxenes (Czank and Liebau, 1980; Czank and Simons, 1983; Ried, 1984; Angel et al., 1984; Angel, 1986b; Veblen, 1985a). Structural disorder is so prevalent in the tetravalent manganese oxides that even basic structure determinations of many of these minerals have been extraordinarily difficult (Burns and Burns, 1979). Structural disorder is common in the series containing schafarzikite, versiliaite, and apuanite (Mellini et al., 1981; Ferraris et al., 1986) and has recently been reported to be common in the bixbyite-braunite polysomatic series (de Villiers and Buseck, 1989).

Slabs of pyroxene and spinel structure can be used to

describe sapphirine and surinamite (Moore and Araki, 1983; Barbier and Hyde, 1988), as well as rhönite and other minerals related to aenigmatite (Bonaccorsi et al., 1990), and polysomatic disorder corresponding to slabs of surinamite in sapphirine has been observed by Christy and Putnis (1988).

It is thus clear that polysomatic structures can, and in many cases do, possess structural disorder based on missing or extra polysomatic slabs. In addition, it is common to find two minerals in the same polysomatic series occurring in parallel intergrowths. Mineralogists and petrologists who deal with these structures therefore should be aware of this potential for structural disorder and its consequences, such as causing nonstoichiometry in rock-forming minerals.

Chemical relationships among polysomes

One message of the polysomatic model is that the members of a polysomatic series must be stoichiometrically collinear with respect to the numbers and types of crystallographic sites (Thompson, 1978). A corollary of this principle is that the stoichiometries of crystals with polysomatic structural disorder also will fall on a mixing line between the two end-member structures. Thompson (1981a) showed several petrologically oriented examples of how this collinearity and the chemical coplanarity of intersecting polysomatic series can be used to simplify complex composition spaces. The reader is referred to that paper.

From the mineralogical perspective, it is sometimes of interest to evaluate the chemistry of structurally disordered materials. Although it is now possible to analyze very small regions (~100 Å diameter) directly with analytical transmission electron microscopy, a much more accurate assessment of the ratios of the various crystallographic sites in a disordered (or ordered) region of a crystal can be obtained by applying the polysomatic model to HRTEM images. An example involving disordered pyriboles was given by Veblen and Buseck (1979), and another example comparing site ratios with TEM analyses in disordered pyroxene-pyroxenoid mixtures was given by Livi and Veblen (1987b). For pyriboles, what is commonly observed from HRTEM data is the widths of a sequence of silicate chains in the structure. These can be factored into M and P slabs by converting each single chain to one P slab, each double chain to one M slab and one P slab, each triple chain to two M slabs and one P slab, etc. The number of M slabs and P slabs are then summed, and for ferromagnesian pyriboles the chemical composition is given by $[N_M \cdot (Mg,Fe)_3Si_4O_{10}(OH)_2] + [N_P \cdot (Mg,Fe)_4Si_4O_{12}]$, where the numbers of slabs are multiplied by the compositions of the two types of slabs. It is essential to scale the formulae of the two slabs properly. In the above expression, the M-slab composition looks like a normal Mg-Fe talc formula, but the composition of the P slab is a multiple of the normal three- or six-O atom pyroxene formula. It is obvious that the formulae that are used for the slabs depend on how the slabs are chosen.

Polyhedral distortions and chemical partitioning

From the last section, it is clear that the polysomatic model can be used to calculate mineral stoichiometries, even in disordered structures. But can it be used to predict the details of polyhedral distortions and chemical partitioning in polysomatic structures? It was shown in the section on pyroxenoids that the P-slab regions of pyroxenoids are quite similar to the analogous parts of the clinopyroxene structure, but does this similarity extend down to the scale of individual coordination polyhedra? How does the ability of the polysomatic model to predict polyhedral distortions and cation partitioning trends compare with that of other models for modular crystals, such as the crystallographic shear model?

Polyhedral distortions. One way to assess whether the polysomatic model can predict the geometrical details of coordination polyhedra is to compare the distortions of structurally analogous polyhedra in several different structures from a single polysomatic series. This can be done using the simple parameters Δ and σ (Table 3), which measure variations in bond distance and bond angle, respectively, within a polyhedron (Robinson et al., 1971). Table 3 shows these polyhedral distortion parameters for both the tetrahedra and octahedra in the ferromagnesian biopyriboles talc (Tc; Perdikatsis and Burzlaff, 1981), jimthompsonite (Jt; Veblen and Burnham, 1978), anthophyllite (At; Finger, 1970; bond distances and angles calculated by Hawthorne, 1983), and orthopyroxene (Px; Burnham et al., 1971). In this group of structures, the following polyhedra are analogous in the polysomatic model:

$$T_{Px} = T2_{At} = T3_{Jt}$$
$$M1_{Px} = M2_{At} = M4_{Jt}$$
$$M2_{Px} = M4_{At} = M5_{Jt}$$
$$T_{Tc} = T1_{At} = T1,T2_{Jt}$$
$$M_{Tc} = M3,M1_{At} = M1,M2,M3_{Jt}.$$

The polyhedral distortion parameters in Table 3 indicate that the tetrahedra in the M slabs of these structures are all very regular, with Δ values less than 0.5 and σ^2 no greater than 2.2. The tetrahedra of all the P slabs, however, are much more distorted, with Δ = 1.06–3.03 and σ^2 = 16.6–30.1. Similarly, the octahedral sites of the M slabs all possess Δ values below 1.95, but sites analogous to M1 of pyroxene are characterized by a larger spread of metal-oxygen distances, with Δ = 4.12–4.58; however, these octahedral sites all have similar values for σ, which are dominated by the octahedral flattening caused by edge sharing. On the other hand, the polyhedra analogous to M2 of pyroxene are highly distorted in all of these polysomes, with much higher values of both Δ and σ than any of the other polyhedra.

The polyhedral distortion parameters of Table 3 show that the polysomatic model can be used to predict the

TABLE 3. Polyhedral distortion parameters for orthopyroxene, anthophyllite, jimthompsonite, and talc

	P-slab sites			M-slab sites		
	T	M2	M1	T	M	
Px*	$\Delta = 1.77, \sigma^2 = 16.6$**	$\Delta = 91.77, \sigma^2 = 188.0$	$\Delta = 4.12, \sigma^2 = 27.4$			
	$\Delta = 2.97, \sigma^2 = 29.3$					
At	$\Delta = 1.44, \sigma^2 = 30.1$	$\Delta = 171.46, \sigma^2 = 214.3$	$\Delta = 4.58, \sigma^2 = 30.7$	$\Delta = 0.48, \sigma^2 = 0.7$	$\Delta = 0.22, \sigma^2 = 44.8$	At
	$\Delta = 1.06, \sigma^2 = 18.0$			$\Delta = 0.22, \sigma^2 = 0.1$	$\Delta = 1.95, \sigma^2 = 34.6$	
Jt	$\Delta = 3.03, \sigma^2 = 27.3$	$\Delta = 148.62, \sigma^2 = 447.9$	$\Delta = 4.35, \sigma^2 = 28.1$	$\Delta = 0.08, \sigma^2 = 0.1$	$\Delta = 0.08, \sigma^2 = 31.4$	Jt
	$\Delta = 1.34, \sigma^2 = 18.1$			$\Delta = 0.08, \sigma^2 = 0.3$	$\Delta = 0.37, \sigma^2 = 33.9$	
				$\Delta = 0.11, \sigma^2 = 2.2$	$\Delta = 0.86, \sigma^2 = 28.0$	
				$\Delta = 0.21, \sigma^2 = 1.7$		
				$\Delta = 0.01, \sigma^2 = 0.0$	$\Delta = 0.42, \sigma^2 = 28.6$	Tc
				$\Delta = 0.00, \sigma^2 = 0.0$	$\Delta = 0.27, \sigma^2 = 28.6$	

* Px = orthopyroxene, At = anthophyllite, Jt = jimthompsonite, Tc = talc.

** $\Delta = \left\{ \sum_{i=1}^{n} [(r_i - r_m)/r_m]^2/n \right\} \times 10^4$, where r_i = individual bond lengths, r_m = mean bond length, n = number of bonds in coordination polyhedron; $\sigma^2 = \sum_{i=1}^{n} (\theta_i - \theta_m)^2/(n-1)$, where θ_i = individual bond angle, θ_m = ideal bond angle, n = number of bond angles in the coordiantion polyhedron (Robinson et al., 1971).

likely degrees of distortion in the coordination polyhedra of a polysome, once the distortions in other polysomes are known. What is not shown by these simple distortion parameters is that the detailed geometries of coordination polyhedra are reproduced fairly accurately in all of these structures; the tetrahedra corresponding to the P slabs are all distorted in very much the same way, for example. The polysomatic model thus can be used to predict even the details of polysomatic structures.

How well are such structural details predicted by other models of modular structures, such as the crystallographic shear and chemical twinning models? As it turns out, these other models are very poor at predicting the details of polyhedral distortions. For example, the CS model for deriving amphibole from pyroxene shears the pyroxene M2 site into an amphibole M3-site position (Chisholm, 1975), thus implying no difference between the highly regular and highly distorted sites. Similarly, the CS model cannot be used to draw any conclusions about the differing distortions of the P- and M-slab tetrahedra, since the distorted tetrahedra of the pyroxene structure are replicated to form all the tetrahedra of amphibole, jimthompsonite, etc. The chemical twinning model likewise is not very useful for understanding the detailed polyhedral distortions in the region of the "twin" plane, as shown by the major structural reorganization implied by the ideal twinned structure of Figure 8a and the real structures shown in Figures 8b and 8c. This is not to say that the CS and chemical twinning models are not useful, but, if one is interested in subtle structural details, the polysomatic model is clearly superior.

Why is this so? The success of the polysomatic model in this respect stems from the fact that the slab modules preserve at least nearest-neighbor coordination relationships and in most cases even the polyhedral linkages from polysome to polysome, whereas the other models do not. Since it is these close-range characteristics that dominate the distortions of coordination polyhedra, the polysomatic model can predict these subtleties.

Chemical partitioning. The distribution of cations among the various crystallographic sites of a structure depends, to a first approximation, on the geometries of the coordination polyhedra. Since the geometries of cation sites of a polysomatic slab can remain much the same throughout a polysomatic series, as shown in the last section, it follows that the partitioning of cations should be fairly consistent throughout a polysomatic series. This is, indeed, the case for polysomatic series in which the cation partitioning behavior has been determined.

An excellent example of the consistency of cation distributions across a polysomatic series is the partitioning of Fe and Mg in the ferromagnesian biopyriboles. It is common knowledge that the larger, more distorted sites invariably possess a higher Fe/Mg ratio than the more regular octahedral sites in pyroxenes (M2 enriched in Fe; Virgo and Hafner, 1969; Papike and Cameron, 1980), amphiboles (M4; Hafner and Ghose, 1971; Hawthorne, 1983), chesterite (MT5 and MD4), and jimthompsonite (M5; Veblen and Burnham, 1978). These systematics of cation partitioning also apply to the chemistry of individual sites in coexisting biopyriboles. Thus, the compositions of coexisting anthophyllite, chesterite, jimthompsonite, and talc are consistent with the identical partitioning of cations among the sites of the M and P slabs throughout the series (see Veblen, 1981b, Fig. 7). Similarly, Livi and Veblen (1987b) have used analytical electron microscopy to show that there is a linear relationship between chemical composition and the P/(P + W) ratio in the replacement of the calcium manganese pyroxene johannsenite by manganese pyroxenoids, even in highly disordered intergrowths in which the mixing of the pyroxene, rhodonite, and pyroxmangite structures is on the unit-cell scale.

The compositional coherency observed in polysomatic

series provides a method for simplifying and predicting the compositions of compounds in a polysomatic series whenever the number of chemical components exceeds the number of structural components. As an example, in the simplest ferromagnesian biopyribole system there are three independent compositional components, such as En = $Mg_4Si_4O_{12}$, Tc = $Mg_3Si_4O_{10}(OH)_2$, and the exchange component FM = $FeMg_{-1}$. However, there are only two structural components with distinct stoichiometries (M and P). If we assume that the partitioning of cations in analogous sites is identical throughout the polysomatic series, then we can simplify the compositional representation of the series to only two components, specifically the compositions of the end-member pyroxene and sheet silicate.

Although the assumption of equal occupancies in analogous sites and compositional collinearity throughout a polysomatic series may be good to a first approximation, it clearly will not be exactly correct. Just as there are minor variations in the geometries of analogous coordination polyhedra in different polysomes (e.g., the octahedra in Figs. 14a and 14b), at least minor differences in cation partitioning also should be expected. However, these relationships may prove useful in many polysomatic series.

Polysomatism and reactions

Solid-state reactions occur in numerous petrogenetic processes, and an understanding of their mechanisms is therefore important to the geological sciences. A very common type of solid-state reaction is one in which the solid reactant and product(s) belong to the same polysomatic series. Reactions of this sort include the oriented replacement of pyroxene by amphibole, wide-chain pyriboles, and sheet silicates during alteration or weathering; oriented replacement of amphibole by pyroxene during prograde metamorphism; and numerous reactions in which one sheet silicate replaces another during diagenesis, metamorphism, alteration, or weathering.

It is important to note that geologically important solid-state reactions commonly involve a fluid phase in addition to the solid reactants and products. This is in keeping with the definition of Schmalzried (1981), who states that "a solid state chemical reaction in the classical sense occurs when local transport of matter is observed in crystalline phases. This definition does not mean that gaseous or liquid phases may not take part in solid state reactions. However, it does mean that the reaction product occurs as a solid phase. Thus, the tarnishing of metals during dry or wet oxidation is considered to be a solid state reaction."

There are several important aspects of solid-state reactions in the earth sciences. Here I will consider the structural mechanisms of such reactions and the nature of the chemical transport that is an integral part of them. Reaction kinetics are related intimately to these two aspects but will not be considered here specifically.

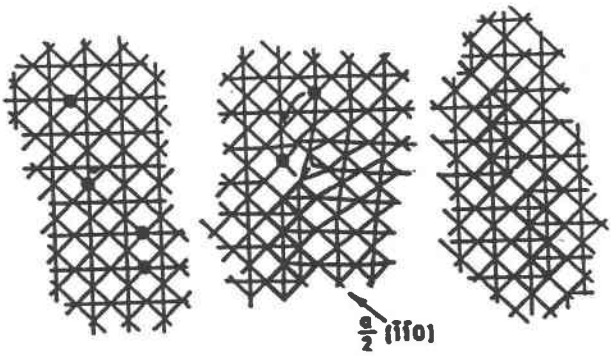

Fig. 19. A mechanism for the formation of CS planes by reduction of WO_3 (Anderson and Hyde, 1967). The CS planes grow by actual shearing of the parent structure at an advancing partial dislocation. O vacancies (represented by black circles) diffuse to and condense on the advancing shear plane. (From Anderson, 1972.)

Structural mechanisms of reactions

Just as there are several ways of describing modular crystal structures, there are different ways of describing the mechanism of a solid-state reaction. Ideally, one would like to state the path that every atom takes from one structure to the other, as well as the paths of atoms that diffuse or flow to or from the reaction site. Such atomistic descriptions, however, typically cannot be verified experimentally in complex materials such as minerals. Testable descriptions of reaction mechanisms commonly rely, therefore, on an understanding of defects that are formed and propagate as a necessary part of the reaction. Such defects may include various types of dislocations, which may form the terminus of an advancing planar defect such as a CS plane or a stacking fault. However, it is commonly overlooked that some solid-state reactions can occur via the motion of a line defect that forms the edge of a polysomatic defect. Such a line defect can involve virtually no net displacement or strain of the surrounding structure.

One of the early motivations behind the crystallographic shear model for planar defects was the recognition that the reactions that produce such defects truly may involve shearing of the parent structure (Anderson, 1972). Figure 19 illustrates one model (Anderson and Hyde, 1967) that shows how CS planes can form in the WO_3 structure by an actual shearing operation, and it is now well established that such shear is the predominant mechanism for their formation during reduction reactions in this structure type (e.g., Iijima, 1975). The slab of sheared structure expands by the advance of its "tip" or edge, which is a line defect that can be described as a partial dislocation. The same is true of CS planes and platelet defects formed by reduction of initially stoichiometric rutile (Bursill and Hyde, 1972; Bursill et al., 1984). The CS model obviously is an excellent way to view structures produced in this fashion, since it describes not only the structure of the reaction product but also the

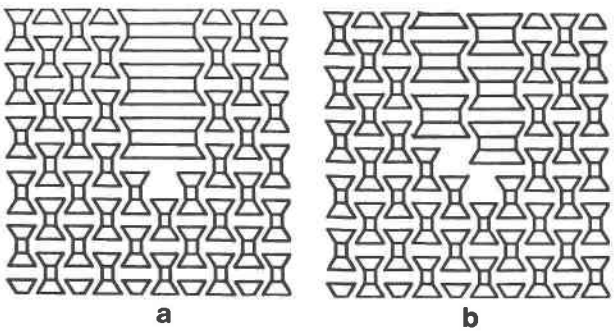

Fig. 20. Two common mechanisms of polysomatic replacement reactions in pyroxene. (**a**) Three single-chain I-beams are replaced by one triple-chain I-beam: PPPP → PMMP. (**b**) Four single-chain I-beams are replaced by two double-chain I-beams: PPPPP → PMPMP. These mechanisms are typical of pyribole replacement mechanisms in that they involve negligible net shear of the reactant structure. (From Veblen, 1981b.)

mechanism of the reaction that produces it. Note, however, that the atomistic aspects of these reduction reactions (i.e., the precise mechanisms of formation and migration of O vacancies) are still not fully resolved, despite extensive experiments and speculation (Tilley, 1987).

On the other hand, many structures that can be described by a CS model seldom if ever form by a structural shearing mechanism: amphibole can grow of its own accord, without resorting to shearing of a preexisting pyroxene. Furthermore, there are many systems in which defects that can be described by a CS model form, but by a reaction mechanism that does not involve crystallographic shear. The same is true for structures that can be described by chemical twinning: they seldom if ever form by glide twinning of a preexisting structure.

Figure 20 shows two ways in which pyroxene is commonly replaced by hydrous pyriboles. These reaction mechanisms can be described simply as the replacement of pyroxene by slabs having a polysomatic sequence different from that of pyroxene. In Figure 20a, the sequence PPPP is replaced by PMMP (a slab of triple-chain structure one chain wide), and in Figure 20b, PPPPP is replaced by PMPMP (a slab of amphibole structure two chains wide). These two structural mechanisms are typical of pyribole replacement reactions in that they do not involve shearing of the reactant structure. On the other hand, the introduction of a single M slab into pyroxene, which has been observed only rarely, does involve a net displacement of the pyroxene structure across the slab; the termination of the slab can be described as a partial dislocation having a Burgers vector of either $\frac{1}{2}[\mathbf{b} + \mathbf{c}]_{px}$ or $\frac{1}{2}[\mathbf{a} + \mathbf{c}]_{px}$. This uncommon reaction mechanism is analogous to the crystallographic shearing mechanism shown in Figure 19. While polysomatic reactions in chain silicates commonly involve minimal strain of the reactant crystal, it should be noted that those in sheet silicates commonly do involve shear. For example, replacement reactions involving micas and chlorite typically involve considerable local changes in volume and distortion of the crystal in the neighborhood of the reaction site (Veblen and Ferry, 1983; Eggleton and Banfield, 1985; Maresch et al., 1985).

Since the reaction of a single M slab into pyroxene can be described as the propagation of a dislocation, it can be argued that the introduction of two M slabs can be described as the introduction of two dislocations. The Burgers vectors of the two dislocations sum to a whole lattice translation (or alternatively can be thought of as having opposite sign), and hence there is no net displacement. In fact, not only the material in the cores of the dislocations, but also all of the material between them, is completely reconstructed in these reactions. For the case of the reaction PPPPP → PMPMP, a slab of structure approximately 13 Å wide is essentially dissolved and rebuilt. Using the polysomatic description of the reaction given in the last sentence, one can very simply describe with a high degree of accuracy the initial structure and the structure following the reaction. The dislocation description, however, is not only more complex but also does not indicate much about the details of the final structure. This author therefore believes that the polysomatic description of the reaction mechanism is superior. In fact, any information about net structural displacements (i.e., a nonzero net Burgers vector) is inherently included in such a description.

That alternative descriptions can be applied to a polysomatic reaction is also illustrated by transformations in the pyroxene-pyroxenoid system. It has been shown in both synthetic (Angel et al., 1984; Angel, 1986b) and natural materials (Veblen, 1985a) that pyroxene can transform to pyroxenoid by the formation of faults parallel to $\{11\bar{1}\}_{px}$. Angel et al. (1984) and Angel (1986b) described the mechanism of these reactions as the motion of dislocations having a Burgers vector of $\frac{1}{4}[2\bar{3}\,\bar{1}]$ or its equivalent. Although such a description may convey the structural displacement across some of the faults formed in the transformations, it is incomplete in that it does not define the structure resulting from reaction, i.e., it does not adequately define the initial and final states. Reactions in this system alternatively can be described using the polysomatic model, for example, PPPPP → PWPWP (a slab of pyroxene becoming a block of rhodonite structure) or PPPPPP → PWPPWP (a slab of pyroxene becoming a block of pyroxmangite structure). Whereas HRTEM suggests that both of these reactions are common in the alteration of johannsenite to pyroxenoids (Veblen, 1985a), the reaction PPP → PWP, corresponding to the passage of a single dislocation through the structure, is less common and results in stacking faults that connect the terminations of isolated W slabs. Note that the polysomatic descriptions uniquely define the starting structure and the final structure that results from reaction, but the structural displacements involved in the reaction are also implicit in these descriptions. Each W slab involves a displacement that is equivalent to that of a partial dislocation, for example, with the Burgers vector of Angel et al. (1984).

The polysomatic description of such reactions thus conveys far more information than a simple dislocation description.

Biopyribole and pyroxenoid replacement reactions also illustrate the pitfalls of atomistic-scale descriptions of solid-state reactions. For example, Dent Glasser and Glasser (1961) suggested that rhodonite transforms to wollastonite by means of a set of simple hops by Si atoms, whereas the rest of the structure is preserved. We now know from electron microscopy that the transformation is highly reconstructive, involving major structural rearrangements whether they are described by a dislocation model (Angel et al., 1984) or the polysomatic model (Veblen, 1985a). The seductiveness of atom-by-atom descriptions of reaction mechanisms has also led to the proposal that silicate chains polymerize by a set of very simple atomic hops during the replacement of one biopyribole by another (Nakajima and Ribbe, 1981). Unfortunately, careful examination of the whole structures involved in these reactions shows that this mechanism requires major diffusion of octahedrally coordinated cations right through the silicate layers that supposedly remain essentially intact. Furthermore, it is inconsistent with experimentally determined structures for the terminations of polysomatic slabs that form by reaction (e.g., Veblen and Buseck, 1980), which indicate that the silicate layers do not remain continuous during such reactions. Although atomistic models are attractive and surely have their place, I would urge that their use be restricted to simpler structures. In polysomatic reactions, the larger structural modules commonly can be observed with HRTEM experiments, and the coarser-scale polysomatic description therefore seems to be the most useful.

Chemical transport associated with polysomatic reactions

Because they involve the replacement of one type of structural slab with another having a different stoichiometry, polysomatic reactions involve the diffusion of various chemical components to and away from the reaction site, or both. Indeed, one can deduce the reaction stoichiometry from the structural mechanism of the reaction observed with HRTEM by applying the formalism discussed in the section "Chemical relationships among polysomes." If the chemical compositions of the reactant and product are also known, then one can write a detailed reaction that shows which components must be added or subtracted during the reaction (e.g., that are supplied or removed by a metamorphic fluid). Examples of this method of calculating the fluid/solid mass balances have been given for reactions involving the replacement of biotite by chlorite and vice versa (Veblen and Ferry, 1983; Eggleton and Banfield, 1985; Maresch et al., 1985).

Because the chemical transport involved in polysomatic reactions may control the reaction kinetics, it is important to understand its mechanism. It is possible that in some polysomatic reactions the chemical transport occurs by bulk diffusion (sometimes called lattice diffusion), which involves the migration of point defects through the reactant structure. However, it has also been suggested that most transport in polysomatic reactions occurs by pipe diffusion along the structural channels that can occur at the terminations of growing polysomatic slabs of reaction product (e.g., Veblen and Buseck, 1980). In some cases, these channels may be organized into a grain boundary separating the reactant and product structures along a reaction front. Although slab terminations may not always involve large channels, there necessarily will be some kind of zone of structural disruption, and there is experimental HRTEM evidence that relatively large channels (culverts?) do occur in many cases.

The need for an alternative to bulk diffusion can be appreciated by noting the extremely sluggish bulk diffusion rates in many silicates. For example, topotaxic reactions in which pyroxenes are replaced by other biopyriboles require substantial diffusion of octahedrally coordinated cations, yet they can proceed by alteration at temperatures on the order of 500 °C (or even during weathering: Eggleton and Boland, 1981). If we assume Arrhenius behavior from experimental temperatures above 1000 °C down to 500 °C, then the average Ca-Mg binary interdiffusion coefficients of Brady and McCallister (1983) yield a diffusion coefficient $\tilde{D} = 1.6 \times 10^{-27}$ cm^2/s at 500 °C. Applying the simple expression $x = (Dt)^{1/2}$ to estimate the range over which a diffusion process is effective (e.g., Putnis and McConnell, 1980; x = distance, D = diffusion coefficient, t = time), we find that the diffusion distance at this temperature is only about 20 Å in 10^6 yr. Although this diffusion distance may seem to be very small, it is, in fact, consistent with blocking temperatures for cation ordering in pyroxenes between 400 and 500 °C. (e.g., Mueller, 1969). Since relatively long-range diffusion is necessary in biopyribole alteration, such a short diffusion distance clearly implies that the transport mechanism cannot be bulk diffusion through the chain silicate structure.

The likely alternative to bulk diffusion in polysomatic reactions is that the chemical transport takes place along the linear defect at the termination of the advancing lamella of reaction product (or along the grain boundary, if the reaction occurs via the motion of a two-dimensional reaction front). Because the free apertures associated with the line defects at the terminations of growing lamellae commonly are as large or larger than those associated with the channels in many zeolite structures, Veblen and Buseck (1980) suggested that the rates of diffusion associated with polysomatic reactions may be similar to those found in zeolites, where the time scales for diffusion in some cases are measured in minutes or seconds, even at room temperature.

Diffusion rates in zeolites vary widely from structure to structure (Barrer, 1971, 1978), but generally they are much larger than those of silicates with less-open structures. Indeed, even room-temperature coefficients for some diffusing species in some zeolites may be 10 or more orders of magnitude larger than diffusion coefficients for

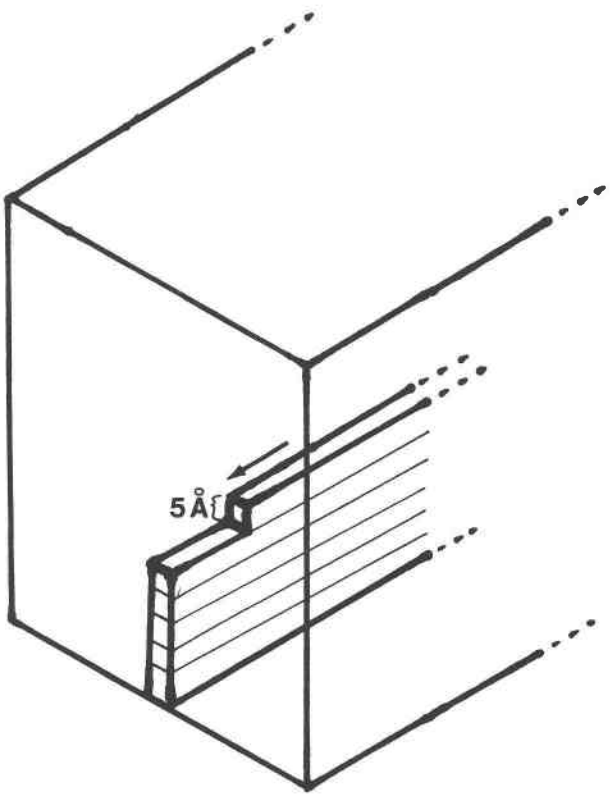

Fig. 21. Schematic diagram of the geometry of polysomatic replacement reactions. A growing slab of product structure advances by migration of a jog in the line defect at its termination in the direction of the arrow. Each reaction step results in the conversion of material corresponding to the height of only one jog, which in chain silicates is less than 5 Å.

clinopyroxene at 1100 °C. Choosing the tracer diffusion coefficient for H_2O in chabazite (Barrer and Fender, 1961; diffusion coefficients for H_2O are similar to those for monovalent cations), which as a free aperture of 3.7 × 4.2 Å, and again assuming Arrhenius behavior, we can calculate $D^* = 4.0 \times 10^{-4}$ cm²/s at 500 °C. Although not directly comparable to the average interdiffusion coefficient for clinopyroxene given above (tracer diffusion coefficients are close to intrinsic diffusion coefficients for the same species—see Brady, 1975, p. 976), this value is more than 22 orders of magnitude larger, and one can do much with 22 orders of magnitude. Indeed, the time scale associated with a diffusion distance of 1 mm is only about 30 s for this diffusion coefficient. This is not surprising, since industrial processes involving cation exchange and molecular sieving, which rely on diffusion into zeolite channels, occur in real time.

Although it can be argued that diffusion along the channels at the edges of polysomatic lamellae is very rapid and zeolitelike, relying on such diffusion for replacement reactions is geometrically inefficient; rather than taking place throughout the structure, all the diffusion for a growing polysomatic slab is localized along a single line, which moves as the lamella grows. This geometry is illustrated in Figure 21, which schematically shows a slab of reaction product forming by migration (in the direction of the arrow) of a jog in the line defect that defines the lamellar termination. In chain silicates, the height of such jogs is only about 4.5 Å, so that lamellae of the reaction product can only advance that far for each reaction step. Is zeolitelike diffusion rapid enough for this inefficient process to work? If we assume that diffusion is the rate-limiting step in such a reaction, that each reaction step advances a growing lamella by 5 Å, that the diffusion distance associated with the reaction is 1 mm (e.g., the distance between fractures that act as sources and sinks for components required and produced by the reaction), and that the time characteristic of this distance is 30 s, then it will take the lamella approximately 2 yr to advance 1 mm. This is a very short time for most geological processes. In fact, we know that alteration and retrograde reactions in biopyriboles commonly are sluggish enough so that they do not go to completion even with extremely slow cooling rates. This suggests that diffusion may not be as rapid as in zeolites, that jogs along the channels leading to the reaction site may cause the diffusion rate to decrease, or that diffusion is not always the rate-controlling step.

I confess readily that the above argument is fraught with inexactness. A correct treatment of the diffusion problem would not use a simple diffusion distance and would have to take into account the fact that the reaction site is essentially a moving point that acts as a source or sink, or both, for the diffusing species. Tracer and interdiffusion coefficients cannot be compared directly. There is much variation in zeolite diffusion rates, and although diffusion coefficients used here are appropriate for monovalent cations and H_2O, the coefficients for divalent cations are somewhat smaller. The channels along which the diffusion takes place must contain jogs, and there is no obvious way to assess the effects of such jogs on diffusion rates. Despite these obvious objections, however, these simple considerations provide a permissive argument that rapid diffusion along channels at the terminations of polysomatic slabs may be the primary mechanism by which diffusion occurs in polysomatic reactions. This is fortunate, since bulk diffusion clearly is not a viable mechanism for many such reactions.

Given the likelihood that the dominant diffusion mechanism in polysomatic reactions is rapid pipe diffusion along structural tunnels, we should consider the possibility that such diffusion shares aspects other than rapidity with zeolites. For example, molecular (and ionic) sieving is common in zeolites. Such sieving could lead to ionic activities at replacement reaction sites that are substantially different from those outside a reacting crystal. Molecular sieving also could occur along grain boundaries active in a reaction.

Conclusions

This paper has reviewed several aspects of polysomatism. Although the notions of polysomes and polysomat-

ic series are not the only approaches to modular crystal structures and their relationships, they do provide a powerful tool for describing many structures that are alternatively described by several different models, such as crystallographic shear, chemical twinning, and intergrowth. Furthermore, the polysomatic viewpoint has several advantages over other ways of viewing structures that contain two-dimensional modules. In some cases, it can be used to predict the details of polyhedral distortions and chemical partitioning across an entire polysomatic series. Many examples of structural disorder in minerals can be described simply as various types of aperiodicity in the arrangement of polysomatic slabs, and at least some structural disorder of this sort has been observed in virtually every polysomatic series that has been investigated with transmission electron microscopy. Finally, many solid-state reactions involve the replacement of one polysome by another of the same polysomatic series. For such reactions, the polysomatic description of the structural reaction mechanisms indicates not only the displacements of the reactant structure, but also the detailed structures of the reactant and solid product and their relationship. The line defects at the terminations of growing polysomatic lamellae are necessarily zones of disrupted structure and commonly are structural channels. These channels probably provide rapid pathways for the diffusion that is an essential part of polysomatic reactions.

Acknowledgments

I am indebted to polysomatism's inventor, J.B. Thompson, Jr., from whom I first heard the magical terms M and P. I hope that in this paper I have not twisted his original intent beyond recognition. I also am indebted to C.W. Burnham and P.R. Buseck, collaborators on much of the early work that provided some of the ideas presented in this paper. The present state of my education was completed by my students who have worked on modular structures, notably J.F. Banfield, G.D. Guthrie, Jr., P.J. Heaney, K.J.T. Livi, and E.A. Smelik. Thanks also are due to G.D. Price, who first urged me to write a review of polysomatism, albeit for another journal, and to P.B. Moore, who provided a lively review of this paper. The ideas presented here evolved through a succession of NSF grants, the most recent of which is EAR-8903630, and were first presented as a lecture at a symposium honoring Professor Thompson's many contributions, held at Harvard in September, 1989.

Permission for reproduction of Figures 4, 6, 17, and 19 has been granted by the Royal Society of Chemistry, London; for Figure 5 by Oxford University Press, Oxford, United Kingdom and by Academic Press, Duluth, Minnesota; for Figure 7b by Blackie, Glasgow; for Figure 7c by the International Union of Crystallography, Chester, United Kingdom; for Figures 8 and 9 by the Fourth Division of the Science Council of Japan, Tokyo; and for Figure 16 by Oxford University Press, Oxford, United Kingdom.

References cited

Amouric, M., Gianetto, I., and Proust, D. (1988) 7, 10 and 14 Å mixed-layer phyllosilicates studied structurally by TEM in pelitic rocks of the Piemontese zone (Venezuela). Bulletin de Minéralogie, 104, 298–313.

Anderson, J.S. (1972) Shear structures and non-stoicheiometry. Surface and Defect Properties of Solids, 1, 1–55.

Anderson, J.S., and Hyde, B.G. (1967) On the possible role of dislocations in generating ordered and disordered shear structures. Journal of Physics and Chemistry of Solids, 28, 1393–1408.

Andersson, S., and Hyde, B.G. (1974) Twinning on the unit cell level as a structure-building operation in the solid state. Journal of Solid State Chemistry, 9, 92–101.

Angel, R.J. (1986a) Polytypes and polytypism. Zeitschrift für Kristallographie, 176, 193–204.

——— (1986b) Transformation mechanisms between single-chain silicates. American Mineralogist, 71, 1441–1454.

Angel, R.J., and Burnham, C.W. (1991) Pyroxene-pyroxenoid polysomatism revisited: A clarification. American Mineralogist, 76, 900–903.

Angel, R.J., Price, G.D., and Putnis, A. (1984) A mechanism for pyroxene-pyroxenoid transformations. Physics and Chemistry of Minerals, 10, 236–243.

Angel, R.J., Price, G.D., and Yeomans, J. (1985) Energetics of polytypic systems: Further applications of the ANNNI model. Acta Crystallographica, B41, 310–319.

Bailey, S.W. (1984) Micas. Mineralogical Society of America Reviews in Mineralogy, 13, 1–584.

——— (1988) Hydrous phyllosilicates (exclusive of micas). Mineralogical Society of America Reviews in Mineralogy, 1–785.

Bailey, S.W., Frank-Kamenetskii, V.A., Goldsztaub, S., Kato, A., Pabst, A., Schulz, H., Taylor, H.F.W., Fleischer, M., and Wilson, A.J.C. (1977) Report of the International Mineralogical Association (IMA)–International Union of Crystallography (IUCr) Joint Committee on Nomenclature. Acta Crystallographica, A33, 681–684.

Banfield, J.F., Karabinos, P., and Veblen, D.R. (1989) Transmission electron microscopy of chloritoid: Intergrowth with sheet silicates and reactions in metapelites. American Mineralogist, 74, 549–564.

Banfield, J.F., Veblen, D.R., and Jones, B.F. (1990) Transmission electron microscopy of subsolidus oxidation and weathering of olivine. Contributions to Mineralogy and Petrology, 106, 110–123.

Barbier, J., and Hyde, B.G. (1988) Structure of sapphirine: Its relation to the spinel, clinopyroxene and β-gallia structures. Acta Crystallographica, B44, 373–377.

Barrer, R.M. (1971) Intracrystalline diffusion. In Molecular sieve zeolites—II, p. 1–36. American Chemical Society Advances in Chemistry Series 102, Washington, DC.

——— (1978) Zeolites and clay minerals as sorbents and molecular sieves. Academic Press, London.

Barrer, R.M., and Fender, B.E.F. (1961) The diffusion and sorption of water in zeolites—II. Intrinsic and self-diffusion. Journal of Physics and Chemistry of Solids, 21, 12–24.

Bonaccorsi, E., Merlino, S., and Passero, M. (1990) Rhönite: Structural and microstructural features, crystal chemistry and polysomatic relationships. European Journal of Mineralogy, 2, 203–218.

Bovin, J.-O., and O'Keeffe, M. (1981) Electron microscopy of oxyborates. II. Intergrowth and structural defects in synthetic crystals. Acta Crystallographica, A37, 35–42.

Bovin, J.-O., O'Keeffe, M., and O'Keefe, M.A. (1981a) Electron microscopy of oxyborates. I. Defect structures in the minerals pinakiolite, ludwigite, orthopinakiolite, and takéuchiite. Acta Crystallographica, A37, 28–35.

——— (1981b) Electron microscopy of oxyborates. III. On the structure of takéuchiite. Acta Crystallographica, A37, 42–46.

Brady, J.B. (1975) Reference frames and diffusion coefficients. American Journal of Science, 275, 954–983.

Brady, J.B., and McCallister, R.H. (1983) Diffusion data for clinopyroxenes from homogenization and self-diffusion experiments. American Mineralogist, 68, 95–105.

Breck, D.W. (1974) Zeolite molecular sieves, 771 p. Wiley and Sons, New York.

Burnham, C.W., Clark, J.R., Papike, J.J., and Prewitt, C.T. (1967) A proposed crystallographic nomenclature for clinopyroxene structures. Zeitschrift für Kristallographie, 125, 1–6.

Burnham, C.W., Ohashi, Y., Hafner, S.S., and Virgo, D. (1971) Cation distribution and atomic thermal vibrations in an iron-rich orthopyroxene. American Mineralogist, 56, 850–876.

Burns, R.G., and Burns, V.M. (1979) Manganese oxides. In Mineralogical Society of America Reviews in Mineralogy, 6, 1–46.

Burns, R.G., Burns, V.M., and Stockman, H.W. (1985) The todorokite-buserite problem: Further considerations. American Mineralogist, 70, 205–208.

Bursill, L.A., and Hyde, B.G. (1972) Crystallographic shear in the higher

Ti oxides: Structure, texture, mechanisms and thermodynamics. Progress in Solid State Chemistry, 7, 177–253.

Bursill, L.A., Blanchin, M.G., and Smith, D.J. (1984) Precipitation phenomena in non-stoichiometric oxides II. {100} platelet defects in reduced rutiles. Proceedings of the Royal Society of London, A391, 373–391.

Buseck, P.R., and Veblen, D.R. (1988) Mineralogy. In P.R. Buseck, J.M. Cowley, and L. Eyring, Eds., High-resolution transmission electron microscopy, p. 308–377. Oxford University Press, Oxford, United Kingdom.

Cameron, M., and Papike, J.J. (1979) Amphibole crystal chemistry: A review. Fortschritte der Mineralogie, 57, 28–67.

Chisholm, J.E. (1973) Planar defects in fibrous amphiboles. Journal of Materials Science, 8, 475–483.

——— (1975) Crystallographic shear in silicate structures. Surface and Defect Properties of Solids, 4, 126–151.

——— (1981) Pyribole structure types. Mineralogical Magazine, 44, 205–216.

Christy, A.G., and Putnis, A. (1988) Planar and line defects in the sapphirine polytypes. Physics and Chemistry of Minerals, 15, 548–558.

Czank, M., and Liebau, F. (1980) Periodicity faults in chain silicates: A new type of planar lattice fault observed with high resolution electron microscopy. Physics and Chemistry of Minerals, 6, 85–93.

Czank, M., and Simons, B. (1983) High resolution electron microscopic studies on ferrosilite III. Physics and Chemistry of Minerals, 9, 229–234.

Dent Glasser, L.S., and Glasser, F.P. (1961) Silicate transformations: Rhodonite-wollastonite. Acta Crystallographica, 14, 818–822.

Eggleton, R.A., and Banfield, J.F. (1985) The alteration of granitic biotite to chlorite. American Mineralogist, 70, 902–910.

Eggleton, R.A., and Boland, J.N. (1981) Weathering of enstatite to talc through a sequence of transitional phases. Clays and Clay Minerals, 30, 11–20.

Eyring, L. (1988) Solid-state chemistry. In P.R. Buseck, J.M. Cowley, and L. Eyring, Eds., High-resolution transmission electron microscopy, p. 378–476. Oxford University Press, Oxford, United Kingdom.

Ferraris, G., Mellini, M., and Merlino, S. (1986) Polysomatism and the classification of minerals. Rendiconti Società Italiana di Mineralogia e Petrologia, 41, 181–192.

Finger, L.W. (1970) Refinement of the crystal structure of an anthophyllite. Carnegie Institution of Washington Year Book, 68, 283–288.

Freed, R.L., and Peacor, D.R. (1967) Refinement of the crystal structure of johannsenite. American Mineralogist, 52, 709–720.

Frost, H.J., Ashby, M.F., and Spaepen, F. (1980) Tilt boundaries in hard-sphere F.C.C. crystals. In Grain boundary structure and kinetics, p. 149–153. American Society for Metals, Metals Park, Ohio.

Giovanoli, R. (1985) A review of the todorokite-buserite problem: Implications to the mineralogy of marine manganese nodules: Discussion. American Mineralogist, 70, 202–204.

Golden, D.C., Dixon, J.B., and Chen, C.C. (1986) Ion exchange, thermal transformations, and oxidizing properties of birnessite. Clays and Clay Minerals, 34, 511–520.

Guinier, A., Bokij, G.B., Boll-Dornberger, K., Cowley, J.M., Durovic, S., Jagodzinski, H., Krishna, P., de Wolff, P.M., Zvyagin, B.B., Cox, D.E., Goodman, P., Hahn, Th., Kuchitsu, K., and Abrahams, S.C. (1984) Nomenclature of polytype structures, report of the International Union of Crystallography Ad-Hoc Committee on the Nomenclature of Disordered, Modulated and Polytype Structures. Acta Crystallographica, A40, 399–404.

Guthrie, G.D., Jr., and Veblen, D.R. (1989) High-resolution transmission electron microscopy of mixed-layer illite/smectite: Computer simulations. Clays and Clay Minerals, 37, 1–11.

——— (1990) Interpreting one-dimensional high-resolution transmission electron micrographs of sheet silicates by computer simulation. American Mineralogist, 75, 276–288.

Hafner, S.S., and Ghose, S. (1971) Iron and magnesium distribution in cummingtonites $(Fe,Mg)_7Si_8O_{22}(OH)_2$. Zeitschrift für Kristallographie, 133, 301–326.

Hawthorne, F.C. (1983) The crystal chemistry of the amphiboles. Canadian Mineralogist, 21, 173–480.

——— (1985) Towards a structural classification of minerals: The $^{VI}M^{IV}T_2\Phi_n$ minerals. American Mineralogist, 70, 455–473.

Hazen, R.M., and Finger, L.W. (1981) Module structure variation with temperature, pressure, and composition: A key to the stability of modular structures? In M. O'Keeffe and A. Navrotsky, Eds., Structure and bonding in crystals, vol. II, p. 109–116. Academic Press, New York.

Hussain, A., and Kihlborg, L. (1976) Intergrowth tungsten bronzes. Acta Crystallographica, A32, 551–557.

Hutchison, J.L., Irusteta, M.C., and Whittaker, E.J.W. (1975) High resolution electron microscopy and diffraction studies of fibrous amphiboles. Acta Crystallographica, A31, 794–801.

Hyde, B.G. (1976) Rutile: Planar defects and derived structures. In H.-R. Wenk, Ed., Electron microscopy in mineralogy, p. 310–318. Springer-Verlag, Berlin.

Iijima, S. (1975) High-resolution electron microscopy of crystallographic shear structures in tungsten oxides. Journal of Solid State Chemistry, 14, 52–65.

Johannsen, A. (1911) Petrographic terms for field use. Journal of Geology, 19, 317–322.

Kitamura, M., Shen, B., Banno, S., and Morimoto, N. (1984) Fine textures of laihunite, a nonstoichiometric distorted olivine-type mineral. American Mineralogist, 69, 154–160.

Kohn, J.A., and Eckart, D.W. (1965) Mixed-layer polytypes related to magnetoplumbite. American Mineralogist, 50, 1371–1380.

Koto, K., Morimoto, N., and Narita, H. (1976) Crystallographic relationships of the pyroxenes and pyroxenoids. Journal of the Japan Association of Mineralogists, Petrologists, and Economic Geologists, 71, 248–254.

Kunze, V.G. (1961) Antigorit. Fortschritte der Mineralogie, 39, 206–324.

Law, A.D., and Whittaker, E.J.W. (1980) Rotated and extended model structures in amphiboles and pyroxenes. Mineralogical Magazine, 43, 565–574.

Liebau, F. (1985) Structural chemistry of silicates, 347 p. Springer-Verlag, Berlin.

Livi, K.J.T., and Veblen, D.R. (1987a) "Eastonite" from Easton, Pennsylvania: A mixture of phlogopite and a new form of serpentine. American Mineralogist, 72, 113–125.

——— (1987b) Analytical electron microscopy (AEM) of a pyroxene-to-pyroxenoid reaction. Eos, 68, 453.

Makovicky, E. (1989) Modular classification of sulphosalts—current status: Definition and application of homologous series. Neues Jahrbuch für Mineralogie Abhandlungen, 160, 269–297.

Maresch, W.V., and Czank, M. (1983) Problems of compositional and structural uncertainty in synthetic hydroxyl-amphiboles; with an annotated atlas of the realbau. Periodico di Mineralogia–Roma, 52, 463–542.

——— (1988) Crystal chemistry, growth kinetics and phase relationships of structurally disordered (Mn^{2+},Mg)-amphiboles. Fortschritte der Mineralogie, 66, 69–121.

Maresch, W.V., Massonne, H.-J., and Czank, M. (1985) Ordered and disordered chlorite/biotite interstratifications as alteration products of chlorite. Neues Jährbuch für Mineralogie Abhandlungen, 152, 79–100.

Megaw, H.D. (1973) Crystal structures: A working approach, 563 p. W.B. Saunders, Philadelphia.

Mellini, M., Amouric, M., Barronnet, A., and Mercuriot, G. (1981) Microstructures and non-stoichiometry in schafarzikite-like minerals. American Mineralogist, 66, 1073–1079.

Mellini, M., Ferraris, G., and Compagnoni, R. (1985) Carlosturanite: HRTEM evidence of a polysomatic series including serpentine. American Mineralogist, 70, 773–781.

Mellini, M., Trommsdorff, V., and Compagnoni, R. (1987) Antigorite polysomatism: Behavior during progressive metamorphism. Contributions to Mineralogy and Petrology, 97, 147–155.

Moore, P.B. (1986) Quartz: Variations on a theme. American Mineralogist, 71, 540–546.

Moore, P.B., and Araki, T. (1974) Pinakiolite, $Mg_2Mn^{3+}O_2[BO_3]$; warwickite, $Mg(Mg_{0.5}Ti_{0.5})O[BO_3]$; wightmanite, $Mg_5(O)(OH)_5[BO_3])\cdot nH_2O$: Crystal chemistry of complex 3 Å wallpaper structures. American Mineralogist, 59, 985–1004.

Moore, P.B., and Araki, T. (1983) Surinamite, ca. $Mg_3Al_4Si_3BeO_{16}$: Its crystal structure and relation to sapphirine, ca. $Mg_{2.8}Al_{7.2}Si_{1.2}O_{16}$. American Mineralogist, 68, 804–810.

Moore, P.B., Shen, J., and Araki, T. (1985) Crystal chemistry of the $^{2}_{\infty}[M^{3+}{}_{2}\phi_{2}(TO_4)_2]$ sheet: Structural principles and crystal structures of ruizite, macfallite and orientite. American Mineralogist, 70, 171–181.

Moore, P.B., Sen Gupta, P.K., Schlemper, E.O., and Merlino, S. (1987) Ashcroftine, ca. $K_{10}Na_{10}(Y,Ca)_{24}(OH)_4(CO_3)_{16}(Si_{56}O_{140})\cdot 16H_2O$, a structure with enormous polyanions. American Mineralogist, 72, 1176–1189.

Mueller, R.F. (1969) Kinetics and thermodynamics of intracrystalline distributions. In J.J. Papike, Ed., Pyroxenes and Amphiboles: Crystal Chemistry and Phase Petrology, Mineralogical Society of America Special Paper, 2, 83–93.

Müller, W.F., and Wenk, H.-R. (1978) Mixed-layer characteristics in real humite structures. Acta Crystallographica, A34, 607–609.

Nakajima, Y., and Ribbe, P.H. (1980) Alteration of pyroxenes from Hokkaido, Japan, to amphibole, clays and other biopyroboles. Neues Jahrbuch für Mineralogie Monatshefte, 1, 258–268.

——— (1981) Texture and structural interpretation of the alteration of pyroxene to other biopyriboles. Contributions to Mineralogy and Petrology, 78, 230–239.

Ohashi, Y., and Finger, L.W. (1975) Pyroxenoids: A comparison of refined structures of rhodonite and pyroxmangite. Carnegie Institution of Washington Year Book, 74, 564–569.

O'Keefe, M.A. (1984) Electron image simulation: A complementary processing technique. In Electron optical systems, p. 209–220. SEM Inc., AMF O'Hare, Chicago.

O'Keeffe, M., and Andersson, S. (1977) Rod packings and crystal chemistry. Acta Crystallographica, A33, 914–923.

O'Keeffe, M., and Hyde, B.G. (1985) An alternative approach to nonmolecular crystal structures, with emphasis on the arrangements of cations. Structure and Bonding, 61, 77–144.

Olives Baños, J. (1985) Biotites and chlorites as interlayered biotite-chlorite crystals. Bulletin de Minéralogie, 108, 635–641.

Papike, J.J., and Cameron, M. (1976) Crystal chemistry of silicate minerals of geophysical interest. Reviews of Geophysics and Space Physics, 14, 37–80.

——— (1980) Crystal chemistry of silicate pyroxenes. In Mineralogical Society of America Reviews in Mineralogy, 7, 5–92.

Pauling, L. (1929) The principles determining the structures of complex ionic crystals. Journal of the American Chemical Society, 51, 1010–1026.

Perdikatsis, B., and Burzlaff, H. (1981) Strukturverfeinerung am Talk $Mg_3[(OH)_2Si_4O_{10}]$. Zeitschrift für Kristallographie, 156, 177–186.

Pinckney, L.R., and Burnham, C.W. (1988) Effects of compositional variation on the crystal structures of pyroxmangite and rhodonite. American Mineralogist, 73, 798–808.

Portier, R., Carpy, A., Fayard, M., and Galy, J. (1975) Perovskite-like compounds ABO_{3+x} ($0.44 \leq x \leq 0.5$). Electron microscopy survey on the $(Na,Ca)_nNb_nO_{3n+2}$ ($4 < n \leq 4.5$) homologous series. Physica Status Solidi, A30, 683–697.

Post, J.E., and Appleman, D.E. (1988) Chalcophanite, $ZnMn_3O_7\cdot 3H_2O$: New crystal-structure determinations. American Mineralogist, 73, 1401–1404.

Post, J.E., and Bish, D.L. (1988) Rietveld refinement of the todorokite structure. American Mineralogist, 73, 861–869.

——— (1989) Rietveld refinement of the coronadite structure. American Mineralogist, 74, 913–917.

Post, J.E., and Veblen, D.R. (1990) Crystal-structure determinations of synthetic sodium, magnesium, and potassium birnessite using TEM and the Rietveld method. American Mineralogist, 75, 477–489.

Post, J.E., Von Dreele, R.B., and Buseck, P.R. (1982) Symmetry and cation displacements in hollandites: Structure refinements of hollandite, cryptomelane and priderite. Acta Crystallographica, B38, 1056–1065.

Prewitt, C.T. (1980) Pyroxenes. Mineralogical Society of America Reviews in Mineralogy, 7, 1–525.

Price, G.D. (1983) Polytypism and the factors determining the stability of spinelloid structures. Physics and Chemistry of Minerals, 10, 77–83.

Price, G.D., and Yeomans, J. (1984) The application of the ANNNI model to polytypic behavior. Acta Crystallographica, B40, 448–454.

——— (1986) A model for polysomatism. Mineralogical Magazine, 50, 149–156.

Putnis, A., and McConnell, J.D.C. (1980) Principles of mineral behavior, 257 p. Elsevier, New York.

Reynolds, R.C., Jr., (1980) Interstratified clay minerals. In G.W. Brindley and G. Brown, Eds., Crystal structure of clay minerals and their X-ray identification, ch. 3. The Mineralogical Society, London.

——— (1988) Mixed layer chlorite minerals. In Mineralogical Society of America Reviews in Mineralogy, 19, 601–629.

Ried, H. (1984) Intergrowth of pyroxene and pyroxenoid; chain periodicity faults in pyroxene. Physics and Chemistry of Minerals, 10, 230–235.

Robinson, K., Gibbs, G.V., and Ribbe, P.H. (1971) Quadratic elongation: A quantitative measure of distortion in coordination polyhedra. Science, 172, 567–570.

Schmalzried, H. (1981) Solid state reactions, 254 p. Verlag Chemie, Weinheim.

Self, P.G., and O'Keefe, M.A. (1988) Calculation of diffraction patterns and images for fast electrons. In P.R. Buseck, J.M. Cowley, and L. Eyring, Eds., High-resolution transmission electron microscopy, p. 244–307. Oxford University Press, Oxford, United Kingdom.

Smith, J.V. (1977) Enumeration of 4-connected 3-dimensional nets and classification of framework silicates, I. Perpendicular linkage from simple hexagonal net. American Mineralogist, 62, 703–709.

——— (1978) Enumeration of 4-connected 3-dimensional net and classification of framework silicates, II. Perpendicular and near-perpendicular linkages from 4.8^2, 3.12^2 and 4.6.12 nets. American Mineralogist, 63, 960–969.

——— (1979) Enumeration of 4-connected 3-dimensional nets and classification of framework silicates, III. Combination of helix, and zigzag, crankshaft and saw chains with simple 2D nets. American Mineralogist, 64, 551–562.

Spinnler, G.E. (1985) HRTEM study of antigorite, pyroxene-serpentine reactions, and chlorite, 248 p. Ph.D. thesis, Arizona State University, Tempe, Arizona.

Takéuchi, Y. (1978) "Tropochemical twinning": A mechanism of building complex structures. Recent Progress of Natural Sciences in Japan, 3, 153–181.

Takéuchi, Y., Haga, N., Kato T., and Miura, Y. (1978) Orthopinakiolite, $Me_{2.95}O_2[BO_3]$: Its crystal structure and relationship to pinakiolite, $Me_{2.90}O_2[BO_3]$. Canadian Mineralogist, 16, 475–485.

Thompson, J.B., Jr. (1970) Geometrical possibilities for amphibole structures: Model biopyriboles. American Mineralogist, 55, 292–293.

——— (1978) Biopyriboles and polysomatic series. American Mineralogist, 63, 239–249.

——— (1981a) An introduction to the mineralogy and petrology of the biopyriboles. In Mineralogical Society of America Reviews in Mineralogy, 9A, 141–188.

——— (1981b) Polytypism in complex crystals: Contrasts between mica and classical polytypes. In M. O'Keeffe and A. Navrotsky, Eds., Structure and bonding in crystals II, p. 167–196. Academic Press, New York.

Tilley, R.J.D. (1980) Non-stoicheiometric crystals containing planar defects. Surface and Defect Properties of Solids, 8, 121–201.

——— (1987) Defect crystal chemistry, 236 p. Blackie, Glasgow.

Turner, S., and Buseck, P.R. (1979) Manganese oxide tunnel structures and their intergrowths. Science, 203, 456–458.

——— (1981) Todorokites: A new family of naturally occurring manganese oxides. Science, 212, 1024–1027.

——— (1983) Defects in nsutite (γ-MnO_2) and dry-cell battery efficiency. Nature, 304, 143–146.

Turner, S., and Post, J.E. (1988) Refinement of the substructure and superstructure of romanechite. American Mineralogist, 73, 1155–1161.

Van Landuyt, J., Amelinckx, S., Kohn, J.A., and Eckart, D.W. (1974) Multiple beam direct lattice imaging of the hexagonal ferrites. Journal of Solid State Chemistry, 9, 103–119.

Veblen, D.R. (1981a) Amphiboles and other hydrous pyriboles—Mineralogy. Mineralogical Society of America Reviews in Mineralogy, 9A, 1–372.

——— (1981b) Non-classical pyriboles and polysomatic reactions in biopyriboles. In Mineralogical Society of America Reviews in Mineralogy, 9A, 189–236.

——— (1983) Microstructures and mixed layering in intergrown wonesite, chlorite, talc, biotite, and kaolinite. American Mineralogist, 68, 566–580.

——— (1985a) TEM study of a pyroxene-to-pyroxenoid reaction. American Mineralogist, 70, 885–901.

——— (1985b) High-resolution transmission electron microscopy. In Mineralogical Association of Canada Short Course Handbook, 11, 63–90.

Veblen, D.R., and Burnham, C.W. (1978) New biopyriboles from Chester, Vermont: II. The crystal chemistry of jimthompsonite, clinojimthompsonite, and chesterite, and the amphibole-mica reaction. American Mineralogist, 63, 1053–1073.

Veblen, D.R., and Buseck, P.R. (1979) Chain-width order and disorder in biopyriboles. American Mineralogist, 64, 687–700.

——— (1980) Microstructures and reaction mechanisms in biopyriboles. American Mineralogist, 65, 599–623.

——— (1981) Hydrous pyriboles and sheet silicates in pyroxenes and uralites: Intergrowth microstructures and reaction mechanisms. American Mineralogist, 66, 1107–1134.

Veblen, D.R., and Ferry, J.M. (1983) A TEM study of the biotite-chlorite reaction and comparison with petrologic observations. American Mineralogist, 68, 1160–1168.

Veblen, D.R., and Ribbe, P.H. (1982) Amphiboles: Petrology and experimental phase relations. Mineralogical Society of America Reviews in Mineralogy, 9B, 1–390.

Veblen, D.R., Buseck, P.R., and Burnham, C.W. (1977) Asbestiform chain silicates: New minerals and structural groups. Science, 198, 359–365.

Veblen, D.R., Guthrie, G.D., Jr., Livi, K.J.T., and Reynolds, R.C., Jr. (1990) High-resolution transmission electron microscopy and electron diffraction of mixed-layer illite/smectite: Experimental results. Clays and Clay Minerals, 38, 1–13.

de Villiers, J.P., and Buseck, P.R. (1989) Stacking variations and nonstoichiometry in the bixbyite-braunite polysomatic mineral group. American Mineralogist, 74, 1325–1336.

Virgo, D., and Hafner, S.S. (1969) Fe^{2+},Mg order-disorder in heated orthopyroxenes. Mineralogical Society of America Special Paper, 2, 83–93.

Wadsley, A.D. (1964) Inorganic non-stoichiometric compounds. In L. Mandelcorn, Ed., Non-stoichiometric compounds, p. 98–209. Academic Press, New York.

Warshaw, C.M., and Roy, R. (1961) Classification and a scheme for the identification of layer silicates. Geological Society of America Bulletin, 72, 1455–1492.

White, T.J., and Hyde, B.G. (1982a) Electron microscopy study of the humite minerals: I. Mg-rich specimens. Physics and Chemistry of Minerals, 8, 55–63.

——— (1982b) Electron microscope study of the humite minerals: II. Mn-rich specimens. Physics and Chemistry of Minerals, 8, 167–174.

——— (1983) An electron microscope study of leucophoenicite. American Mineralogist, 68, 1009–1021.

Wuensch, B.J. (1974) Sulfide crystal chemistry. In Mineralogical Society of America Short Course Notes, 1, W21–W44.

Manuscript received January 31, 1990
Manuscript accepted February 19, 1991